EUR 4753 e

COMMISSION OF THE EUROPEAN COMMUNITIES

DESIGN AND CONSTRUCTION OF A 100 KeV ION ACCELERATOR FOR IMPLANTATION STUDIES

edited by

F. CAPPELLANI

Contributors

R. ADAM
R. BENOIT
G. BERTOLINI
F. CAPPELLANI
G. GAGGERO
C. KOCHLER
G. MELANDRONE
C. MONGINI-TAMAGNINI
G. RESTELLI
L. STANCHI

1972

Joint Nuclear Research Centre
Ispra Establishment - Italy

Technology/Electronics

LEGAL NOTICE

This report is on sale at the addresses listed on cover page 4

at the price of B.Fr. 100.–

When ordering, please quote the EUR number and the title, which are indicated on the cover of each report.

Printed by Ceuterick, Louvain
Luxembourg, March 1972

EUR 4753 e

DESIGN AND CONSTRUCTION OF A 100 KeV ION ACCELERATOR FOR IMPLANTATION STUDIES edited by F. CAPPELLANI

Contributors: R. ADAM, R. BENOIT, G. BERTOLINI, F. CAPPELLANI, G. GAGGERO, C. KOCHLER, G. MELANDRONE, D. MONGINI-TAMAGNINI, G. RESTELLI and L. STANCHI

Commission of the European Communities
Joint Nuclear Research Centre — Ispra Establishment (Italy)
Technology/Electronics
Luxembourg, March 1972 — 74 Pages — 36 Figures — B.Fr. 100.–

An ion accelerator has been designed and constructed at the JRC Euratom — Ispra.

Main features of the machine are the following:

— ion energy from some keV to 100 keV for singly ionized atoms; high voltage split in two steps one before and one after the magnet to ensure at least 25 keV extraction potential independently of the energy of the ions on the target;

EUR 4753 e

DESIGN AND CONSTRUCTION OF A 100 KeV ION ACCELERATOR FOR IMPLANTATION STUDIES edited by F. CAPPELLANI

Contributors: R. ADAM, R. BENOIT, G. BERTOLINI, F. CAPPELLANI, G. GAGGERO, C. KOCHLER, G. MELANDRONE, D. MONGINI-TAMAGNINI, G. RESTELLI and L. STANCHI

Commission of the European Communities
Joint Nuclear Research Centre — Ispra Establishment (Italy)
Technology/Electronics
Luxembourg, March 1972 — 74 Pages — 36 Figures — B.Fr. 100.–

An ion accelerator has been designed and constructed at the JRC Euratom — Ispra.

Main features of the machine are the following:

— ion energy from some keV to 100 keV for singly ionized atoms; high voltage split in two steps one before and one after the magnet to ensure at least 25 keV extraction potential independently of the energy of the ions on the target;

EUR 4753 e

DESIGN AND CONSTRUCTION OF A 100 KeV ION ACCELERATOR FOR IMPLANTATION STUDIES edited by F. CAPPELLANI

Contributors: R. ADAM, R. BENOIT, G. BERTOLINI, F. CAPPELLANI, G. GAGGERO, C. KOCHLER, G. MELANDRONE, D. MONGINI-TAMAGNINI, G. RESTELLI and L. STANCHI

Commission of the European Communities
Joint Nuclear Research Centre — Ispra Establishment (Italy)
Technology/Electronics
Luxembourg, March 1972 — 74 Pages — 36 Figures — B.Fr. 100.–

An ion accelerator has been designed and constructed at the JRC Euratom — Ispra.

Main features of the machine are the following:

— ion energy from some keV to 100 keV for singly ionized atoms; high voltage split in two steps one before and one after the magnet to ensure at least 25 keV extraction potential independently of the energy of the ions on the target;

— ion current delivered by a Nielsen source; current intensity of the order of $500/\sqrt{M}$ μA;
— analyzing magnet of sector type with an angle of 127° and radius of 60 cm; double focalization both in the vertical and horizontal plane is provided by means of diverging poles;
— target chamber provided with facilities for implanting at room temperature, high (800 °K) and low (100 °K) temperature, and for bombarding in channeling conditions;
— a beam sweeping system allowing to scan the beam across the target in the vertical and horizontal direction to obtain uniform ion implanted distribution.

Detailed characteristics of the accelerator parts are given in the text together with experimental results obtained in the machine set up. Methods and computing programs developed for ion trajectories calculations used in the design of the accelerator are presented.

— ion current delivered by a Nielsen source; current intensity of the order of $500/\sqrt{M}$ μA;
— analyzing magnet of sector type with an angle of 127° and radius of 60 cm; double focalization both in the vertical and horizontal plane is provided by means of diverging poles;
— target chamber provided with facilities for implanting at room temperature, high (800 °K) and low (100 °K) temperature, and for bombarding in channeling conditions;
— a beam sweeping system allowing to scan the beam across the target in the vertical and horizontal direction to obtain uniform ion implanted distribution.

Detailed characteristics of the accelerator parts are given in the text together with experimental results obtained in the machine set up. Methods and computing programs developed for ion trajectories calculations used in the design of the accelerator are presented.

— ion current delivered by a Nielsen source; current intensity of the order of $500/\sqrt{M}$ μA;
— analyzing magnet of sector type with an angle of 127° and radius of 60 cm; double focalization both in the vertical and horizontal plane is provided by means of diverging poles;
— target chamber provided with facilities for implanting at room temperature, high (800 °K) and low (100 °K) temperature, and for bombarding in channeling conditions;
— a beam sweeping system allowing to scan the beam across the target in the vertical and horizontal direction to obtain uniform ion implanted distribution.

Detailed characteristics of the accelerator parts are given in the text together with experimental results obtained in the machine set up. Methods and computing programs developed for ion trajectories calculations used in the design of the accelerator are presented.

EUR 4753 e

COMMISSION OF THE EUROPEAN COMMUNITIES

DESIGN AND CONSTRUCTION OF A 100 KeV ION ACCELERATOR FOR IMPLANTATION STUDIES

edited by

F. CAPPELLANI

Contributors

R. ADAM
R. BENOIT
G. BERTOLINI
F. CAPPELLANI
G. GAGGERO
C. KOCHLER
G. MELANDRONE
C. MONGINI-TAMAGNINI
G. RESTELLI
L. STANCHI

1972

Joint Nuclear Research Centre
Ispra Establishment - Italy

Technology/Electronics

ABSTRACT

An ion accelerator has been designed and constructed at the JRC Euratom — Ispra.

Main features of the machine are the following:

— ion energy from some keV to 100 keV for singly ionized atoms; high voltage split in two steps one before and one after the magnet to ensure at least 25 keV extraction potential independently of the energy of the ions on the target;

— ion current delivered by a Nielsen source; current intensity of the order of $500/\sqrt{M}$ μA;

— analyzing magnet of sector type with an angle of 127° and radius of 60 cm; double focalization both in the vertical and horizontal plane is provided by means of diverging poles;

— target chamber provided with facilities for implanting at room temperature, high (800 °K) and low (100 °K) temperature, and for bombarding in channeling conditions;

— a beam sweeping system allowing to scan the beam across the target in the vertical and horizontal direction to obtain uniform ion implanted distribution.

Detailed characteristics of the accelerator parts are given in the text together with experimental results obtained in the machine set up. Methods and computing programs developed for ion trajectories calculations used in the design of the accelerator are presented.

KEYWORDS

ACCELERATORS
ION BEAMS
IONS
KEV RANGE 01-10
KEV RANGE 10-100
VALENCE
ION SOURCES
BEAM OPTICS
ION CHANNELING
TARGETS
HIGH TEMPERATURE
TEMPERATURE
PLANNING
ION IMPLANTATION
PROGRAMMING
TRAJECTORIES

PREFACE *)

During the last years there has been a rapid increase of researches concerning the interaction of low energy ion beams with materials. The studies involve either basic research in solid state physics or applied research in electronics, radiation damage, material surface properties etc. Basic researches deal with the investigation of the physico-chemical behaviour in crystalline substrates of ions implanted at energies generally ranging from 10 to 600 keV.
Applied research in electronics concerns mainly the possibility to obtain junctions in semiconductors.

Two years ago, when we started in designing an ion accelerator, some machines appeared on the market, but experiments were performed mainly using mass separators. We decided to construct by ourselves the accelerator because the experience gained would have enabled us to modify the machine any time it was necessary.

The accelerator will be used at the Electronic service for basic researches on properties of materials implanted with different ions and will be put at disposal of people interested in the field of ion implantation.
This machine can be, for instance, utilized in nuclear research applications for the simulation of neutron induced damage in materials.

At the same time that the accelerator was being constructed, techniques for studying the implanted layers have been set up (e.g. Hall effect, authomatic peeling, channelling) which are the necessary complement for such a type of machine.

---

*) Manuscript received on November 9, 1971

The collaboration of many collegues in Ispra has been the determining factor for the success of the project concerning design and construction of the 100 KeV ion accelerator. I wish to thank all this people for their efficient cooperation.

AKNOWLEDGEMENTS

The 100 keV ion accelerator has been accomplished by the joint efforts of many people. Besides the contributors to this report thanks are due to the following people who have especially contributed to the success of the project:
A. Pegoraro for the mechanical design of some parts of the machine;
A. Rota for helpful contribution to the design of the test system and the constant field tube;
C. Ciniselli for contribution in assembling and testing the high voltage supplies;
The main workshop of the C.C.R. Ispra for the construction of the magnet and the mechanical parts of the accelerator;
G. Colombo for the help in the preliminary design of the ion accelerator;
S. Facchetti for contribution in setting up the ion source;
V. Mandl for organization and preliminary leading of the project.

A particular aknowledgement is due to F. Farfalletti-Casali and U. Buzzi for the mechanical design of the whole accelerator and for the engagement in following the assembling of the machine. Their cooperation was of basic importance for the setting up of the ion implanter.

CONTENTS

./.

1. BASIC DESCRIPTION

The schematic layout of the 100 KeV ion accelerator is shown in Fig.1.1 ; Fig.1.2 shows a picture of the machine and Fig.1.3 reports a simplified block diagram demonstrating the operation. As can be seen from this figure, the accelerating voltage has been split in two steps: one before the analyzing magnet and the other following the analyzer.

The voltage V_1 can be set from + 25 KV to + 75 KV in steps of 10 KV while the post-acceleration voltage V_2 can continuously be adjusted from - 25 KV to + 25 KV. The source potential with respect to the target (grounded) , given by the algebraic sum of V_1 and V_2, can be varied from 0 to 100 KV allowing ion energies for singly ionized atoms from 0 to 100 KeV. It is also evident from Fig.1.3 that the minimum extracting voltage for zero beam energy (V_1 = + 25 KV, V_2 = - 25 KV) is still 25 KV. This configuration has two main advantages: high extraction voltage (at least 25 KV) of the ions from the source independently of the final energy of the beam on the target, and definite energy of the ions at the entrance of the magnet (25, 35, 45, 55, 65, 75 KV) thus simplifying magnet calibration.

The ion source is of the Nielsen type producing positive ion beams from a broad range of chemical elements and compounds. Ion beam currents vary, depending on the charge of the source, from some /uA to some hundreds of /uA. The electrostatic focusing system, mounted in the chamber between the magnet and the ion source (acceleration chamber), consists of a set of three cylindrical electrodes (Einzel lens).

The deflection magnet is of the sector type with an angle of 127°, radius 60 cm and a mean gap width of 32 mm. The magnet field can be raised to approximately 8300 Gauss giving mass

analysis up to 160 amu at the maximum energy. Double focalization both in the vertical and the horizontal plane is obtained by means of diverging poles of hyperbolic shape. For the angle of 127° radial and vertical focalization are the same so that a circular beam of parallel trajectories at the input of the magnet is focalized in one point (neglecting space charge effects) at the end of the magnet.

At this point the calculated separation D between two masses of M and M+1 amu is $D = \frac{500}{M}$ mm. At the input and output of the magnet magnetic shunts were necessary to eliminate stray flux effects. At the magnet output, after the shunt, the mass spectra can be visualized by a beam scanner which allows to estimate the separation of the peaks and their resolution.

The postaccelerating system consists of a set of 10 circular electrodes suitably insulated one with respect to the other. The voltage between each electrode and the following is equal to 1/10 of the total accelerating or decelerating potential. The number, distance and shape of the electrodes have been calculated to give a constant electric field distribution on the axis of the chamber in order to avoid, also in the case of retarding potential, defocusing of the ion beam. The measurements performed have confirmed that either accelerating or retarding the ions, there is no remarkable variation of the beam dimensions at the target. The beam sweeping system consists of two pairs of parallel plates placed at 90° one with respect to the other for scanning the beam across the target chamber in the vertical and horizontal direction. The plates are driven by triangular waveforms of 20 and 2000 Hz frequency respectively. The maximum target coverage is a square of three cm. side for 100 KeV ions.

The target chamber is provided with four different terminal flanges which can be easily removed and changed. The first one supports a rotating disc, movable from outside, which allows to hold up to 8 samples for room temperature implants.
The second one allows to warm up to 800° K up to four samples by means of an electron gun; the third flange is provided with facilities to cool down the target to 77° K. A fourth one supports a two axis goniometer which allows target orientation for implantation in channelling conditions.

Except from the ion source and the beam scanners which have been bought from the firm DANFYSIK (Denmark), all parts of the accelerator have been designed and constructed at the C.C.R. Euratom of Ispra.

2. METHODS AND COMPUTING PROGRAMS FOR ION TRAJECTORIES

2.1 Statement of the Problem

The problem which had to be studied and solved consists in setting up a numerical tool, i.e. package of computer programs, apt to determine the trajectories of the ions of a beam produced by the given ion source, in a configuration of the type sketched in Fig.1.1 . The tool has then to be utilized in order to determine and optimize the focalization properties and strength of the considered ion beam on the target, by changing parameters such as: 1) the shape and voltage of the various electrodes in the Einzel lens and in the constant field tube; 2) the radius and aperture angle of the analyzing magnet.

From the computational point of view the problem to be solved may be splitted into three main parts consisting in setting up

the computer programs capable to solve respectively the following problems:

a) calculation of the electrostatic field due to a given electrodes geometric configuration and voltage;

b) the determination of the ion trajectories in the given electrostatic field by taking into account the space charge effect;

c) the determination of the ion trajectories in the magnetic field due to the given analyzing magnet, by taking into account the space charge effect.

The firt two programs must be interconnect due to the fact that the elctrostatic field resulting from the first program is an "input" for the second program. Such couple of programs is used in the calculation of ion trajectories in the acceleration chamber and in the constant field tube. The third program is used to calculate ion trajectories in the analyzing magnet.
The characteristics of the ion beam at the entrance of the magnet and of the constant field tube (beam radius and divergence) are determined by the exit characteristics related respectively to the acceleration chamber and the magnet.

The package of programs has been actually used to perform many parametrical calculations related to the configuration sketched in Fig. 1.1.

However, it is to be noted that the programs are all of them general-purpose and that consequently the package can be used to determine trajectories of charged particles in electrostatic and magnetic fields induced by electrodes configuration also very different from the one here considered, although still in bidimensional geometry.

In the following the characteristics of the mentioned computer programs are described in detail. Besides some computational results obtained by the use of the package of the described programs are shown and discussed.

2.2 Determination of the Electrostatic Field

The problem of determining the electrostatic field induced by a given electrode configuration is brought back, from a mathematical point of view, to that of solving the Laplace equation in the given space, starting by given boundary conditions.
In the case under examination the two-dimensional spaces determined by the coordinates xy and rz were considered. Basically two main directions can be followed to solve the Laplace equation, the one being the use of analytical methods, the other being the adoption of numerical iterative schemes.

The analytical method is used whenever the geometric boundaries of the space considered are originally simple in their shape, or can be brought back to simple shape by the use of a conformal mapping transformation procedure (e.g. when the region is bounded by parallel straight lines). A computer program for IBM 360/65 (1) capable to solve Laplace equation in xy geometry in the case of a boundary configuration constituted by a repeller plate and a system of coaxial slits in multiple parallel electrodes had been set up previously at CETIS. Such a program is based on the Schwarz-Christoffel conformal mapping transformation described in references (2) and (3).
Such a program was used only for calculations related to a source and extraction system with parallel slits which was disregarded in practice in favour of the Nielsen source.

The utilization of numerical iterative methods, to be adopted whenever the boundaries do not present a simple shape or are not easily brought to simple shape by conformal transformation, was thought then to be necessary in the present case.

A program written, at CERN (4) and capable of solving the two dimensional xy and rz Laplace equations by means of finite difference iteration scheme was strongly modified to be adapted to the case in examination, giving so rise to a new program called LESP-MV.
The modification were the following:

a) The possibility of variable mesh distance was introduced. In fact in the case of both the Einzel lens and the constant field tube, there is the necessity to describe particular spatial regions (i.e. near the central axis and the electrodes) by a very great number of points, in order to get values of the electrostatic fields reliable enough for the successive ion trajectories calculations; the use of the program in its original form, i.e. with constant mesh distance, would have rendered enormous the total number of points to be considered, so highly increasing the computer time necessary to fit the required convergence criteria.

b) Double precision was introduced in the iterative scheme to the purpose of getting more precise values of the potential distribution, required in the further calculations.

c) The calculated potentials were memorized in peripheral memories in suitable form to be read by the computer program apt to calculate the ion trajectories in a given electrostatic field.

The so modified program was then finally included in the package of programs utilized for the actual calculation.

2.3 Trajectories of Cherged Particles in Electrostatic Fields

Exact individual particle trajectories may be obtained by solving the equation of motion of a charged particle. The potential map is available on a discrete mesh, obtained as described in § 2.2 .

When a particle is moving in a beam, space charge effects are present and it can no longer be treated independently of the density and distribution of the particles in the beam.

A suitable method for calculation of beams in any type of potential field has been developed by Yokosawa (5). Individual rays from a beam emittance contour are traced simultaneously, assuming, however, that an initially assumed current density distribution j(r) is preserved. Incorporating the space charge term in the manner described by Yokosawa, the motion equation for cylindrical geometries is:

$$\frac{d^2r}{dz^2} = \frac{1+\left(\frac{dr}{dz}\right)^2}{2V}\left[\frac{\delta V}{\delta r} - \frac{dr}{dz}\frac{\delta V}{\delta z} + \frac{I(r)}{2\sqrt{2\pi\varepsilon}\left(\frac{q}{m}\right)^{1/2} V^{1/2}\, r}\right] \quad [1]$$

where:
V is the potential,
q is the charge of the particle,
m is the mass of the particle.

The amount of space charge acting on each individual particle at radius r is proportional to the current I(r) given by:

$$I(r) = I_o\left[\int_o^r rj(r)dr \Big/ \int_o^R rj(r)dr\right]$$

where I_o is the total current and R the maximum radius of the beam. If uniform charge distribution is assumed, I(r) is given by $(r^2/R^2)I_o$.

A computer program, called TRION (6), has been written to integrate numerically the beam equation [1]. A fourth order Runge-Kutta subprogram for simultaneous second-order equations with first derivative performs the integration. The program was made so that, when the marginal ray is crossed by an inner ray, R is assigned to the inner ray. The program reads potential field geometrical data concerning the pattern of the electrodes from a data set produced by LESP-MV program in a previous run. The potential and field components are calculated at each forward integration step from numerically stored potential field by appropriate interpolation formulas. Resulting ray trajectories may be plotted, using a Calcomp plotter, together with the electrode pattern and the map of the potential field (the contour map subprogram COMAP (7) is used).

2.4 Trajectories of Charged Particles in Magnetic Fields

The study was confined to the determination of trajectories of charged particles in the magnetic field produced by an hyperbolic pole shoes magnet. The theory of such a magnet is described in ref. (8). An analytical solution of the motion equation is available only in the absence of space-charge effects.
If space-charge is taken into account the motion equation is no more linear. To derive the motion equation it was assumed that the charges are uniformly distributed in a circular cross-section. This leads to the equation:

$$\frac{d^2r}{ds^2} + \frac{K}{R_o H_o} r - \frac{I_o r_o^2}{2\varepsilon\mu R_o H_o} \frac{1}{r} = 0 \qquad [2]$$

where: s is a coordinate measured on the circular trajectory (beam center-line); r is the radius of the beam; R_o is the radius of the beam center-line; r_o is the radius of the beam at the entrance of the magnet; H_o is the value of the magnetic field (vertical) acting on the beam center-line; K is equal to $\frac{1}{4} \frac{\pi^2}{\alpha^2} \frac{H_o}{R_o}$ where α is the angle of aperture of the magnet.

A computer program, called TRAMA (9), has been written to integrate numerically the beam equation [2]. A fourth order Runge-Kutta sub-program for second order equations performs the integration.

2.5. Some computational results

The package constituted by the three described programs, LESP-MV, TRION, TRAMA was utilized to perform many parametrical calculations related to the accelaration chamber, the analyzing magnet, the constant field tube.

In particular the couple of programs LESP-MV and TRION was utilized for studying the behaviour of the ion beam in the acceleration chamber by changing the geometric configuration and the voltage of the electrodes, and for various ion masses and beam currents.

In fig. 2.1 are reported the equipotential distribution curves for a specific geometry and for the quoted values of the voltage.

In fig. 2.2 the ion trajectories in the ion beam are shown for an ion mass of 84 amu and a beam current of 12 μ A.

As for the magnet the program TRAMA was utilized to study the behaviour of the beam by changing the following prameters:
aperture angle of the magnet
ion mass
ion beam radius at the entrance of the magnet
total beam current

In Fig. 2.3 some plots of the output radius versus current are reported for the quoted values of the above indicated parameters.

Concerning the constant field tube the couple of programs LESP-MV and TRION was utilized for studying various configurations. In Fig. 2.4 the ion trajectories are shown for a decelerating field of 20 KV. The ion mass is 84 amu, the beam current is 12 μA and the energy of entering ions 50 keV. As can be seen from the figure, the beam divergence at the tube entrance is not amplified by the decelerating field.

3. ION SOURCE

3.1. Principle of operation

The oscillating electron source of Nielsen (10) was chosen because of its high versatility. The source is constructed by the firm DANFYSIK whose model 910 is the latest version of the type first described in ref. (10) and has incorporated all improvements made over the years. It has been developped for isotope separator use so giving a high flux of a wide range of ions, from the light gases to the transuranic elements. The maximum current is of the order of $500/\sqrt{M}\ \mu A$ where M is the atomic mass number of the isotope in amu.

The operating principle of the source is the following: a plasma is created in the low pressure gas within the discharge chamber by the electrons emitted from a W or Ta filament; the combined effect of electric and magnetic field causes electrons to spiral so increasing the ionization density.

At the operating pressure the density is sufficiently high that a plasma is maintained producing ions at the rate at which they are extracted as beam current.

The sample material may be introduced in elemental form or as a compound; samples of low vapor pressure can be heated in a crucible or in the case of hardly evaporable materials converted into chlorides by a reaction with carbon tetrachloride vapor which can be admitted to the source (11).

3.2. Source mounting and cooling

The source is mounted on a 10 cm thick and 90 cm in diameter plexiglass disc which provides 100 KV maximum insulation with respect to the acceleration chamber. The source can be moved in any direction in the plane of the disc without breaking vacuum and high voltage by means of four insulated rods (see fig. 4.7 in chp. 4). This facility allows alignement of the source with respect to the Einzel lens-magnet entrance axis when the accelerator is in operation. The beam position can be observed both by the X-Y scanner placed at the output of the accelerating chamber and on a fluorescent screen placed in a suitable control chamber located as shown in fig. 1.1 .

A needle valve driven by an insulated rod is connected to the source and is used for gaseous charges, the gas being put in a glass ball connected to the valve.

Thermocouples are placed on the terminal flange of the source and in contact with the oven. The temperature on the flange when the cooling system is working, does not exceed 70°C also after many hours of source operation. Source cooling is performed using oil for transformers flowing in 3 meters long plastic tubes which act as insulators so that the gear pump for oil circulation is earthed (fig. 3.1). The heat exchangers consist of three glass columns water cooled.

In order to avoid discharges when the accelerator is working at potentials higher than 25 KV, an aluminium cover acting as equipotential surface is placed around the source.

3.3. Electrical supplies

The electrical layout of the source power supply is shown in fig. 3.2. The system is composed by four separate power supplies having the following characteristics:

- Filament 0-25 V 0-60 A D.C.
- Oven 0-25 V 0-50 A A.C.
- Magnet 0-160 V 0-2.5 A D.C.
- Anode 0-160 V 0-5 A D.C.

As the ion plasma into the source is not very sensitive to voltage or current fluctuations of the different source electrodes, no stabilyzing system has been provided.

The system is high voltage insulated by four 130 KV insulating transformers which secondaries are capacitively driven to high voltage potential. This can lead to damage of the diodes with the lowest peak inverse voltage when high voltage discharges occur. In order to avoid this draw-back, selfprotected diodes having a Zener region at 150 V reverse voltage have been used for the filament supply rectifier.

The adjustement of the source electrode voltages or currents is performed by varying the primary voltage of the insulating transformers with variable ratio auto-transformers placed in the control desk.

3.4. Source tests

Using a test system (described in ch. 4) consisting of a 20 KV ion extraction apparatus, an Einzel lens and an analysing magnet, the source has been tested with noble gases as Ar, Kr, Xe; with; B and P and with As.

Working with noble gases the currents extracted from the ion source agreed or exceeded easily the values given by the relation $500 / \sqrt{M}$ μA. For Boron two source charges have been tried. Metallic Boron reacted with CCl_4 yielded quite low current (less than 10 nA), whereas using the mixture KBF_4 + B_2O_3 (8:1 in weight) in the oven, Boron currents of 0.15 μA have been obtained. Anyway also in this last case the yield of Boron ions with respect to the total beam current was low: 3%o.

Phosphor ions have been obtained using a source charge of P_2O_5 in the oven heated at 400°C. The current of P^+ was up to 1.8 μA with a yield of 3% with respect to the total current extracted. Arsenic ion beams have been obtained using $AsCl_3$ or metallic As as charge materials for the ion source. The utilization of Arsine (AsH_3) has been disregarded in order to avoid safety problems. $AsCl_3$ is liquid at room temperature with a vapor pressure of 10 mm at 23°C, and can be handled by using a needle valve. The results obtained indicated a yield of about 7% of As^+ ions after mass separation with respect to the beam current extracted. The mass spectrum showed many spurious peaks due to chlorine and to the extreme reactivity of $AsCl_3$ which exchanges with metals like iron, copper etc... elements appearing in the mass spectrum with currents as high as 1/2 of the As beam.

The best results have been obtained using Arsenic metal. Powdered arsenic metal has been aggregated by compression and charged in the ion source placed in the graphite cylinder of the tetrainlet system which is directly heated by the discharge chamber. Arsenic sublimates at 615°C so that the temperature should be kept well below this point (e.g. 1 mm vapour pressure can be obtained at 372°C); therefore the original quartz tube fitting into the discharge chamber is substituted by another 9 cm long. The yield of As^+ ions obtained was 19% and the mass spectrum appeared extremely clean without spurious masses higher than 1% of the arsenic mass peak. The current of As^+ ions obtainable on the target exceeded easily 1 μA.

4. ACCELERATING SYSTEM AND BEAM FOCUSING

4.1. Preliminary system: general description

A facility working up to 20 KV and consisting of the ion source, extraction and focusing system, magnet analysis and target chamber has been constructed for the following reasons:

- investigation of the operation conditions of a three electrodes (Einzel lens) ion optics to get well defined values of diameter and convergence of the ion beam at the magnet entrance
- experimental determinations of ion trajectories to check the theoretical calculations
- gain of experience in the use of the ion source and of the influence on the ion beam of different parameters as gas pressure, filament type and current etc.
- study of the optimization of the ion source as function of different charge materials.

A schematic layout of the acceleration chamber of the preliminary system is shown in fig. 4.1. Fig. 4.2. is a picture of the end plate of the chamber showing the lens system and the facilities for beam visualisation and current measurements.

Two linear motion feedthroughs are used, the first one carries two insulated crossed wires allowing x - y scanning of the ion beam, the second one moves the Einzel lens along the chamber axis in order to vary the extraction gap from 0 to 50 mm.

The accelerating voltage was supplied to the ion source by a 20 KV Brandenburg generator. The power supply for the ion source is that described in chapter 3, sect. 3.3.

The analysing magnet was of double E type with flat parallel poles. Single focalization on the horizontal plane produced an output beam with elliptic cross section. The distance between the pole shoes was 25 mm; the pole width was 50 mm. The angle was 60° with a 250 mm radius. The maximum magnetic field was 0,7 Wb/m^2 sufficient to deflect a mass of 80 amu at 20 KeV.

The mass resolution was fairly low but sufficient to check the ion beam purity in the measurements for the optimization of the charge material for the ion source. A simple target chamber was placed at the magnet output containing facilities for beam current measurement, and beam visualization.

4.2. Preliminary system: experimental results

The measurements performed can be divided in two groups:

- Investigation of the ion source operation as function of the parameters of the source itself (filament heating

current, anode potential, ion source magnetic field, discharge chamber pressure)

- Study of the influence of the acceleration gap and Einzel lens potential on shape, dimension and homogeneity of the ion beam.

The parameters determined for correct ion source operation are the following:

- filament heating current: 30-35 A (Tungsten filament)
  20-25 A (Tantalum filament)
- anode potential: 75-100 V
- anode current: 0.3-1.5 A
- axial magnetic field: corresponding to a current of 1.5 A in the ion source magnet coil

The gas pressure p in the discharge chamber is optimized by measuring the ion current I after the Einzel lens as function of the needle valve aperture. As indicated in ref. [10] the discharge in the ion source can only exist for p higher than a certain value p_{min}; for $p > p_{min}$ the ion current is nearly independent of p so that the regulation of the needle valve is not critical.

Increasing p, the pressure in the main vacuum system increases leading to increased scattering of the ion beam and then to a slight decrease of the ion current.

Many set of measurements of the beam characteristics have been performed by varying the different parameters involved. Main results are reported in the following.

The dependence of the ion beam diameter on the Einzel lens potential as function of different values of the acceleration gap is shown in fig. 4.3. From the figure it appears that

the dependence of the beam diameter on the acceleration gap is not critical because by varying the voltage of the lens is always possible to obtain a given beam diameter. On the contrary the dependence can be remarkable when it is necessary to obtain at a given point (e.g. at the magnet input) definite conditions of convergence or divergence for the ion trajectories.

Some measurements have been performed with a fixed acceleration gap to determine the value of the Einzel lens voltage necessary to obtain ion trajectories nearly parallel at a given distance from the source output (as required for correct operation of the definitive magnet). Fig. 4.4 shows a set of ion beam diameter determinations performed by inserting in the beam range three visualizers at 30, 64 and 81 cm respectively from the ion source outlet.
In one case the values of the beam diameter calculated as described in ch. 2 are also shown, for comparison. The agreement with the experimental data is fairly good.

In order to check the correct operation of the source and the extraction and focalizing system the homogeneity of the beam has been investigated. Two wires 0,5 mm in diameter placed at 90° mounted insulated on a perspex support were driven by a micrometric linear drive feedthrough placed at 45° with respect to the vertical axis. The wires were connected to two picoamperometers for current measurement.
Fig. 4.5 shows the curves obtained by measuring the current pick up by the horizontal and vertical wires as function of the linear motion feedthrough position. The overlapping of the two curves is not complete; this is due to the beam not exactly centered on the mechanical axis of the accelerator to which is referred the linear drive position. In the figure is also reported the beam cross-section as determined by a square rules fluorescent screen inserted in the same plane of the beam scanner. The curve shapes,

together with the beam section, allow a roughly estimation of the beam homogeneity.

An example of an inhomogeneous ion beam with elliptic cross-section is shown in fig. 4.6. In this case the beam presents a central zone having a higher current density.

4.3. Definitive system

A cross-section of the acceleration chamber and the lens system is shown in fig 4.7.

Materials used are stainless steel and perspex. The insulator between the pumping system and the chamber (necessary when working in the post-acceleration mode) is made of PVC.

The ion source-acceleration chamber system is mounted on a support which allows displacement of the entire assembly in any direction up to 2 cm. The lens system consists, as in the the preliminary assembly, of three cylindrical coaxial electrodes. The first electrode is suitably shaped and acts also as extraction electrode. The lens may be moved from outside along its axis over a range from 0 to 8 cm from the source outlet in order to vary the acceleration gap and then the beam aperture angle.

The first and third electrodes are electrically connected to the chamber walls while the central electrode is at an adjustable high potential. The chamber can be isolated by a gate valve from the rest of the accelerator. No differential pumping for the ion source has been used due to the high pumping speed of the vacuum system adopted.

Vacuum in the acceleration chamber is better than 4×10^{-7} torr; with the source in operation the pressure rises to some 10^{-6} torr.

An X-Y beam scanner is placed between the chamber and the analyzing magnet allowing a careful control of the beam position and shape before it enters the magnet gap. At the magnet entrance the accelerator tube splits into two arms; one follows the poles curvature while the other goes straightforward carrying at its end a small chamber with a movable fluorescent screen and a Faraday cup.
In this way, with the magnet off, it is possible to control if the beam is aligned with the mechanical axis of the system by observing the ion beam position onto the screen and to evaluate the total beam current extracted from the source.

The insulation of the source with respect to the acceleration chamber has been tested with an extraction gap of 6 cm. In these conditions no discharges have been observed up to 130 KV applied voltage. The insulation of the central electrode of the lens system with respect to all the other parts of the chamber has been tested satisfactorily up to 110 KV. All measurements have been performed with different pressures into the vessel from 10^{-6} to 10^{-3} torr, and an ambient relative humidity of 70%.

4.4. High voltage supplies

The accelerating voltage has been conceived divided in two steps: a first voltage supply V_1 (fig. 1.3.) situated before the analysing magnet and a second one, V_2, following the magnet. The requested range of 100 KV can be covered with a fixed voltage of +25 KV or +75 KV and a variable voltage ranging continuously between -25 KV and +25 KV. This allows to enter the magnet with a beam accelerated with a definite voltage so that the calibration of the magnetic field is facilitated. In addition the extraction of the ions is secured with a minimum of 25 KV allowing good extraction of ions from the source even if the final requested energy is definitely lower, i.e. some KeV's. In this case the potential of the

adjustable voltage V_2 is obviously a negative one. In practice the actual realization has been made providing means for switching the fixed voltage to six values: 25, 35, 45, 55, 65 and 75 KV.

In order to fulfill these requirements two power supplies V_1 and V_2 have been constructed. They can be loaded by a current drain up to 1 mA. Both voltages are obtained with regulated power supplies and are connected in series so that only the last one(V_2) is grounded as the target. The stability against load variations is better than one part over 10,000. The reference elements are compensated zener diodes. The reference voltage is directly compared with the high voltage via a bleeder (fig. 4.8). In V_1 voltage supply the current in the bleeder is fixed by resistors R_1, ... R_6 and adjusted to cause the appropriate voltage on a 200 Mohm resistor. The voltage of the virtual ground is compared with an effective ground (apart from an off-set compensation) and amplified in such a sense to drive with negative feed-back a series regulator. The loop is closed via a dc-dc converter which transforms the low voltage to the appropriate voltage by means of a square wave oscillator, a step-up transformer and a rectifier in the quadrupler connection. The voltage quadrupler has been used particularly for reducing the capacitances seen from the primary winding of the transformer.

The variable voltage V_2 (from -25 KV up to +25 KV) has approximately the same schematic (fig. 4.9). Here the bleeder is not directly in series with the reference voltage but is relied to ground. A balanced bridge with the reference voltage is employed to give the virtual ground. For positive high voltages a negative reference voltage is used and viceversa. A unit gain inverter is utilized for reversing the polarity in case of negative voltage. The loop is closed via a dc-dc converter similar to the preceding one but using a voltage doubler. It is clear that the high voltage rectifiers must

be reversed for obtaining negative voltages. This is manually accomplished before operating the device. The reference elements need not to be switched because they contain series diodes so that one of them is always reverse biased. The reference elements and the low voltage control circuits are supplied with a separate regulated power supply.

In fig. 4.10 the block diagram of V_1 is reported. This device supplies both the high voltage positionable in six definite steps from 25 KV to 75 KV and the voltage for the "Einzel lens" which can be positioned in steps of 2% of the output voltage between half and total voltage. Both the step controls are realized by switches driven by motors remotely controlled from the control desk. An ac feed-back has been introduced in the regulated power supply for avoiding relaxation oscillations. The device is protected against overvoltage and overcurrent. The power for the device is taken from the normal 220 V mains via an isolation transformer because all the circuits are isolated from ground being in series to the variable high voltage supply V_2. The device can be energized locally or from the control desk only if there is the permission by the interlock system which is connected to all the doors and enclosures. In addition a mains fall protection circuit utilizing SCR, opens the circuit if the line voltage is lacking even only for one period. This for avoiding inconveniences due to the series of two power supplies.

Voltage supply V_2 has a similar block diagram with the difference that a pole is grounded so that an isolation transformer is not requested. Besides, the voltage adjustment is continuous and manually controlled by a ten turns potentiometer. An inverter is added for negative voltages.

The set-up of both V_1 and V_2 supplies is shown in fig. 4.11.

5. ANALYSING MAGNET

5.1. Magnet design and construction

The analysing magnet has been designed in order to achieve a high ion current yield.

The magnet poles are diverging to allow focalization both in the vertical and horizontal plane. The input beam has to satisfy the following conditions: circular cross-section and parallel ion trajectories.

The design of the magnet has been made keeping the radius as small as possible compared to reasonable values of the induction between the poles in order to reduce dimensions and weight of the magnet. An induction of 1 Wb/m^2 in the iron gap was foreseen; the chosen radius was considered apt to drive onto the target masses up to 240 amu accelerated to 75 KV before the magnet. Successive considerations on the stray flux led to the conclusion that the requested induction in the iron gap caused saturation in other parts of the magnetic circuit. The magnet has been kept with the dimensions indicated in fig. 5.1 and it can be used up to an induction of 083 Wb/m^2 which is sufficient for the ions which are normally used.

Classical considerations on the ion trajectories in uniform magnetic field, neglecting space charge effects, lead to the result that there is a maximum of focalization in the horizontal plane, for an aperture angle of the magnet of 90°. It can be demonstrated (8) that it is possible to have focalization also in the vertical plane; the convergence in the horizontal plane is decreased but not eliminated provided that the percentile decreasing of the induction along the radius be less than the percentile increase of the radius.

If a beam circular cross-section has to be maintained along the trajectory, the vertical and radial focalization must be the same. In order to meet this requirement, the profile of the poles has to be hyperbolic. Assuming that the input trajectories are parallel and focalized in one point at the magnet output, the calculation leads to an aperture angle of $\pi/\sqrt{2}$, that is 127°.

Taking into account the space charge effects, the linear equations which led to the design of the magnet with 127° of aperture, are somewhat modified by a correcting non-linear term. Plots of the trajectories of the ions along the magnet has been obtained by computer elaborations as a function of the beam current intensity. The output beam cross-section can be kept circular also for different angles of aperture if a suitable inclination is given to the input trajectories with respect of the nominal one (convergence for angles of aperture less than 127°); the radius of the output beam cross-section appears to be increasing with the aperture of the magnet. Smaller angles of aperture give a smaller cross-section at the output, i.e. a better focalization, so it can be tempting to decrease this angle. But it is necessary to take into account mass separation. For a selected radius of the nominal trajectory, the mass separation increases with the angle of the magnet. A reasonable estimation can be made for equal mass separation which can be obtained, for smaller angles, increasing the radius of the trajectories by a factor somewhat greater than the ratio between the angles. In conclusion a decrease of the angle of aperture imposes an increase of the radius of the magnet; but the increase of the radius is greater than that given by a direct proportionality so that the length of the path increases. This implies stronger space charge effects and in addition the effect of scattering due to residual gas molecules present in the tube is enhanced. A good criterion of design seems to be the optimization of the mass separation with respect to the length of the trajectories into the iron gap.

It can be demonstrated that there is a flat maximum of the ratio "separation over angle" as a function of the angle. This happens for an angle of 135° but the value of 127° lies still on the flat top of the curve, confirming the goodness of the choice of this angle for the design.

The final magnet has been designed for a nominal angle of aperture of 127° but, taking into account the fringing field effects, the actual angle of the magnet is 123°. The material used is soft iron containing more than 99,5% of iron and less than 0,02% of carbon.

The profile of the pole shoes section should be hyperbolic as obtained solving the equation $xy = NI/K$ where NI is the magnetomotive force and K is a suitable constant of the design. As the part of the hyperbola actually used for the magnet is a very samll one, it is easy to approxiamte closely the curve with an arc of a circus, reducing the difficulties of finishing the surfaces. In practice with a little sacrifice in the desired field pattern, that is in the performance, the profile has been approximated with the rectlinear segment which matches better the theoretical hyperbola in the mean third of the poles section. The maximum deviation from the theoretical curve taking into account the mechanical tolerances resulted to be about 10 microns. The experimental results proved that the magnetic flux distribution in the region of interest is quite satisfactory. The dimension of the section of the gap are reported in fig. 5.4.

The surface of the poles is approximately 1200 cm^2 which gives an attraction force between them of 4800 kg. The inflection of the iron structure results to be negligible even with this considerable force.

The mechanical design comprises a side circular column supporting the coils and two yokes which support the polar pieces and have the shape of a circular sector.

The iron core is composed of five parts rigidly assembled by means of suitable screws made with the same material. All the magnet has a weight of 2,400 kg and rests on three adjustable brass supports.

The ion tube is insulated from the earthed poles by two 3 mm thick PVC spacers.

5.2. Magnet supply

The block diagram of the current supply for the analysing magnet is reported in fig. 5.2. The supply is designed to fulfill the characteristics of the magnet, that is coil resistance 1.38 ohm, maximum magnetic field obtainable at 35 A current.

The supply is current regulated in order to give a very stable magnetic field. The current stability results to be better than 0.2% for variation of the load resistance of a factor 4.

The voltage on a manganon sense resistor caused by the current flowing through the magnet coil is compared with a reference voltage obtained from a temperature compensated Zener diode and used for feedback regulation.

The power is taken from the normal 380 V three-phase mains. The secondary winding of the transformer is connected as six phase star. The power series transistors are cooled with forced air ventilation and are protected against failures of the ventilation circuit. The coil of the magnet is composed of three concentric sections cooled by forced air ventilation. The time constant of the winding is about 2 sec. . The current ripple resulting from the capacitive filtering at the output of the six-phase rectifier and from the time constant of the magnet is less than one part over 10^5.

The current setting can be manually operated locally or from the control desk. The minimum reading on a ten turns potentiometer is one part over 10.000 of the total range.

5.3. Experimental results

The measurements of the field distribution in the iron gap of the analysing magnet and its variation as function of the current supplied to the coils has been performed using a Hall probe induction meter. The probe has been first carefully calibrated by nuclear magnetic resonance techniques.

Fig. 5.3 reports the values of the induction measured in the center of the iron gap as a function of the supply current. Saturation effects appear for currents exceeding 25 A. The induction obtainable without a strong saturation is 0.83 Wb/m^2 which allows to obtain on the target masses up to 160 amu at 100 KeV or in turns the mass 240 at an energy of 75 KeV. Beyond this value obtained with 35 A supply current in the coils of the magnet, a considerable increase of power is required for small increments of induction.

The induction along the gap axis has been measured and found constant within the sensitivity of the gaussmeter (5%o) over the whole length of the pole shoes. At the magnet output, the field measured along the gap axis prolongation decreases by a factor 20 at 10 cm distance for $B < 0.67$ Wb/m^2 (outside saturation region) while for $B > 0.67$ Wb/m^2 the reduction factor is 15. Fig. 5.4 shows a map of the magnetic induction taken in a cross-section of the gap at the center of the magnet for two values of supply current. The data reported refer to saturating and not saturating values of the magnetic field.

The existence of a high stray flux caused a strong bending of the ion trajectories before and after the magnet. To

eliminate this effect, two magnetic shunts have been constructed and placed respectively at the entrance and the output of the magnet. The shunts are two soft iron cylinders 200 mm long and 25 mm thick surrounding the accelerator tube.

The measurements of the magnet resolution have been performed by using the beam scanner placed after the magnet at 250 mm from the pole faces. If D is the distance in mm between two peaks having one mass unit difference, its value has been calculated to be $\frac{500}{M}$ mm (M in amu) at the magnet focus that is at the magnet output.
At the beam scanner the experimentally determined value of D was 6.3 mm determined from the mass spectrum of Xe (from M = 130 to M = 132) displayed with the beam scanner (fig. 5.5).

The resolution R of the current peaks, defined as their full width at half maximum, results from the picture to be of the order of 0.5 mm. These measurements have been performed with a vacuum in the machine of the order of 2×10^{-6} torr; with higher pressures (of the order of 10^{-5} torr) a worsening of the resolution occurs as a result of collisions of the beam particles with residual gas molecules.

In particular processes of ionization and elastic scattering cause the ion trajectories to suffer samll angular deflections giving an increase of the wings and the width of the peaks.

6. CONSTANT FIELD TUBE

The constant field tube design is shown in fig. 6.1. It consists of a set of 10 stainless steel electrodes with a central circular hole suitably shaped and insulated, one

respect to the other, by PVC spacers. A simple modular construction was used wich was easy to build and to modify.

The resistors between the electrodes are put on the external side of the tube and are covered with a perspex tube. The voltage difference between each electrode and the following is equal to 1/10 of the total accelerating or decelerating potential.

The number, dimension and shape of the electrodes have been calculated, as described in chp. 2, to give a constant field distribution on the axis of the tube in order to avoid beam defocusing even in the case of retarding potentials. The measurements performed have confirmed the results of the calculations: no variation of the beam dimensions at the target has been observed varying the postacceleration voltage from -25 KV to +25 KV.

At the constant field tube entrance a stainless steel disc with circular holes ranging from 1 to 22 mm. in diameter acts as collimator for mass separation. The disc can be rotated from outside by an insulated rotary feedthrough.

7. BEAM DEFLECTION AND SWEEPING SYSTEM

At the target the beam has a circular shape with diameters ranging from 2 to 6 mm. In order to implant on the whole slice surface (max. 30 mm in diameter) the ion beam must be sweeped in a linear way along the X and Y axis over the sample area to be implanted. This is carried out in the deflection chamber by means of two pairs of parallel plates placed at 90° one respect to the other. The plates are 10 cm long 6 cm wide; distance between two plates is 2 cm.

The X and Y deflection plates are centered respectively at 76 cm and 63 cm from the target. They are driven by a sweep generator which provides triangular waves with maximum ± 1000 V peak to peak amplitude. The maximum dimension of the sweeped frame will be, for 100 KV accelerated ions, 32 x 38 mm, and the maximum deflection angle is ± 1.5°. The X and Y sweep generators are identical apart the sweeping frequency which is 20 Hz for the X deflection and 2000 Hz for the Y deflection.

Fig. 7.1 shows the block diagram of the system. The wave generator consists of a rectangular wave generator followed by an operational integrator and gives at the output a triangular wave adjustable from 0 to maximum 6.7 volts peak to peak amplitude. This wave is directly amplified up to a maximum of 1000 V peak to peak for the A plates and inverted and amplified in the same way for the B plates. At the amplifiers output the triangular waves are centered on a 500V D.C. level.

The A plates are direct coupled, while the B plates are a.c. coupled to the generator. Potentiometers Px and Py allow shifting the whole frame respectively along the X and Y axis for perfect centering.

A remote control is provided to stop the beam in one angle of the maximum sweeping frame when the desired charge has been implanted. The remote control order is given by the beam current integrator.

8. TARGET CHAMBER

The design of the target chamber for the ion accelerator should satisfy the following requirements:

- the chamber has to accomodate a variety of specimen shape and size

- many specimens must be subsequently irradiated without breaking the vacuum
- ion bombardment must be performed on specimens kept at different temperature from -150°C to some hundreds °C
- the measurement of the beam current on the target must be as accurate as possible
- the vacuum in the target chamber must be of the order of 10^{-6} torr and free from contaminating vapours
- crystalline specimens must be mounted with a definite orientation with respect to the ion beam direction
- the chamber must be easily accessible for servicing
- there should be mounting points for the attachment of accessories, e.g. a beam visualizer, a Faraday cup, ion beam collimators, beam shutter etc... .

It has not been possible to design a single chamber which meets all the above mentioned requirements. Therefore different end flanges have been matched to a chamber which is directly connected to the accelerator and the vacuum apparatus. The chamber is a stainless steel cylinder provided with small flanges for vacuum control, air inlet, Faraday cup insertion and beam shutter.
The chamber can be isolated from the accelerator by a gate valve for servicing without perturbing the vacuum in the machine. Oil vapour free vacuum is provided by a 500 l/s ion pump which allows to obtain ultimate pressures of the order of some 10^{-7} torr.

Facilities interchangable with the standard flange have been designed for respectively: high temperature implantation, liquid nitrogen temperature implantation and implantation in channelling conditions.

Room temperature implantation

The target chamber with the end flange for room temperature implantations is shown in fig. 8.1. Eight positions are available, seven for specimens, one for a beam visualizer that can be observed from the outside of the chamber through a glass window. The specimens up to 25 mm in diameter are placed on sample holders (Dural) mounted on a plexiglass disc. The zone to be implanted is defined by an aperture in the collimator which supports also the secondary electron suppressor; the target acts as the electrode of a Faraday cup so that the measurement of beam current on the target is sufficiently accurate. A spring contact fixed to the plate and pressing the specimen holder is used to measure the current and is connected to the beam integrator. Collimators of variable size and dimensions can be inserted between the beam and the target to define different implantation areas or patterns. Different target holders can be used, e.g. to disorient by a known angle the specimen surface with respect to the ion beam (for bambardment out of channelling).

High temperature implantation

The facility is illustrated in fig. 8.2.

Four specimens can be subsequently irradiated without breaking the vacuum. The specimens are mounted on a rotating disc (stainless-steel) supported on lavite holders placed on tantalum discs which are heated by an electron gun. In this way a temperature of 500°C on the specimen can be obtained in few minutes. The assembly has enough mass to maintain the temperature of the specimen during the implantation time. Otherwise a Boron Nitride disc interposed between specimen and tantalum allows bombardment and contemporary monitoring of the beam current on the target.

The electron gun is at high voltage (6000 V) while the tantalum disc is grounded. Facilities are provided for monitoring target temperature and ion beam current. Collimation of the beam and suppression of the secondary electrons are obtained as previously described for the room temperature base plate.

Low temperature implantation

This facility is shown in fig. 8.3. Four specimens can be subsequently irradiated cooled at about 100°K, without breaking the vacuum in the target chamber. The target specimens are mounted on copper blocks insulated from the supporting rotatable plate. Cooling of the target is achieved by pressing the rear part of the holder on a small liquid nitrogen container. A Boron nitrite spacer assures electrical insulation from the container so that the beam current on the target can be measured. The target temperature is monitored by a thermocouple. Collimation of the beam with secondary electron suppression is obtained as previously indicated.

Facility for target orientation

By placing suitable collimators after the analysing magnet and in the target chamber the ion beam divergence can be considerably reduced; therefore a facility has been designed for bombardment in channeling conditions. In this case by using a supplementary cylinder attached to the target chamber, a two axis goniometer can be fitted to the accelerator. The goniometer was originally designed for atom location experiments using MeV protons or Helium ion beams. It allows target orientation with a precision of 0.05° by proton backscattering techniques. Even in this case facilities are provided for heating or cooling the sample during irradiation. Beam current monitoring is performed in this case by insertion of a Faraday cup since no secondary electron suppression is foreseen for the target itself.

9. VACUUM SYSTEM

Good and clean vacuum are basic requirements for an ion accelerator in order to avoid enlargement of the ion beam due to scattering processes with residual gas molecules and to keep the surface of the samples to be implanted free from hydrocarbon contaminations. This imposes clean vacuum systems capable of ultimate pressures better than 10^{-6} torr in the region of the target together with an appropriate choice of the accelerator materials as stainless steel and perspex.

The vacuum schematic diagram is shown in fig. 9.1. The system is divided by two gate valves G_1 and G_2 into three parts: one for the evacuation of the ion source and the acceleration chamber (A); and the two others for the constant field tube-deflection chamber system (B) and the target chamber respectively (C). This allows to avoid vacuum perturbation in all the accelerator when it is necessary to open a part of the machine.

The vacuum in the first part is obtained by a 3000 l/s oil diffusion pump used in conjunction with a water and a freon cooled traps. A two stages mechanical pump (30 m^3/h) connected to a suitable roots pump are used as backing pumps. They are located underground in order to avoid noise and oil vapours. This forevacuum system is capable to reduce the pressure of the acceleration chamber from the atmospheric pressure to 10^{-2} torr in one minute.

When the ion source is not in operation, the ultimate pressure in the acceleration chamber is 3. 10^{-7} torr; during operation rises to a few times 10^{-6} torr.

A 270 l/s turbomolecular pump is connected to the deflection chamber; when G_1 and G_2 are closed, this pump gives an

ultimate pressure of less than 10^{-6} torr. The target chamber is provided with a 500 l/s ion pump; the forevacuum to start this pump can be supplied by the turbomolecular pump. Ultimate pressure in the target chamber with G_2 closed is of the order of 10^{-7} torr.

10. CONTROL SYSTEMS

The electrical and vacuum commands, controls and protection circuits, as well as the beam control systems are centralized in a desk located in front of the source power supply (fig. 10.1). This latter supports all the instruments at high potential, as V and A meters for the ion source filament, anode, magnet, oven, and indicators for the oven and the source flange temperature. Fig. 10.2 shows a simplified block diagram of the various supply and control units.

10.1. Electrical and vacuum controls

Four variable ratio auto-transformers placed on the control desk allows, as described in chapter 3.4. the variation of currents or voltages of the various ion source electrodes.

The high voltage supplies are remote controlled from the desk. The voltage values can be preselected in six steps of 10 KV from 25 to 75 KV for the first acceleration and continuously varied from 0 to -25 KV or from 0 to +25 KV for the post acceleration voltage.

The Einzel-lens voltage is also remote controlled. This voltage can be varied from 50 to 100% of the first accelerating voltage in 2% steps. Indicators for the actual lens potential are provided.

The current in the analyzing magnet can be regulated from 0 to 35 A by a ten step switch, and fine regulation is performed by a ten turn helipot.

Protections have been provided in order to prevent damaging of the various components of the accelerator. Fig. 10.3 shows a block diagram with the logic of the main protection circuits.

The diffusion pump, the roots, the turbomolecular pump and the ion source are protected against failing of the cooling system by temperature or water pressure sensitive elements which disconnect the power supply of the part without cooling. Indicators allow to localize the failure.

When the pressure in the machine exceeds 10^{-4} torr, the high voltage and the source supply are disconnected. If the pressure exceeds 10^{-2} torr the diffusion pump is automatically stopped. The pump stopping is signalized by ligth indicators.

10.2. Beam control systems

The different systems used for beam control and monitoring are:

- Beam scanners
- Beam current meter and integrator
- Fluorescent beam visualizers

- Beam scanners

Two types of beam scanners are used. One placed at the analyzing magnet entrance which gives the beam position and shape along the X and Y axis is a Danfysik scanner Model 516 with vane probe and position markers Model 571. The position markers give the X and Y axis origin which coincides with the mechanical axis of the accelerating and focusing system.

At the magnet output is placed a Danfysik Model 516 single wire scanner which explores only the X axis and intercepts the beams corresponding to ions of different masses.

Both scanners are driven by a double channel scanner control unit Model 514 A from Danfysik. An oscilloscope which can be switched from one to the other scanner is located in the control desk, for visualization of the beam position and shape at the magnet entrance (fig. 10.4.) and for determination of the different ion masses and magnet resolution (fig. 5.5).

- Beam current meter and integrator

The sample to be implanted acts as the collecting electrode of a Faraday cup as described in chapter 8. This electrode is connected to the current meter and integrator input, so that true ion current can be measured. Integration can then be performed in order to determine the number of ions implanted into the target.

The current meter and integrator is essentially constituted by a transresistance amplifier. A meter measures the output voltage proportional to the input current. The transresistance amplifier is followed by an operational integrator and a voltage level detector with hysteresis. This latter resets the integrator to zero and gives a drive pulse to a mechanical counter any time a predetermined charge has been accumulated.

The number of charges to be implanted can be preset in the counter. At the end of the count-down, integration and, through the remote control switches, beam sweeping are stopped and the beam is deflected out of the target.

A simplified schematic diagram of the current meter and integrator is shown in fig. 10.5.

The current meter has six ranges from 1.5×10^{-10} to 1.5×10^{-5} A full scale. Currents down to 5×10^{-11} A, can be measured with $\pm$ 3% precision.

The charge number can be measured from a minimum of 10^8 to a maximum of 10^{19} charges with the actual meter configuration. Extention of this range can be easily performed if necessary.

- Fluorescent beam visualizer

The fluorescent beam visualizer has been made by depositing a thin uniform layer of potassium bromide (KBr) on a conductive glass disc (12). The glass conductivity is obtained by a treatment with tin chloride vapor ($SnCl_2 - 2H_2O$) as described in ref. (13). The fluorescence of the screen is bright even for beam currents of about 0.5 μ A; however the life time of the screen even if much longer than for screens with ZnS deposits is limited.

- Mass spectrum recorder

In the next future it is foreseen to use a XY recorder for recording the total mass spectrum at the magnet output. This will allow a rapid check of the beam purity and the identification and selection of the ions to be implanted.

The X channel of the recorder will be driven by a voltage signal proportional to the analysing magnet current while a second signal proportional to the beam current after the magnet will be fed to the Y channel.

REFERENCES

(1) A computer program for the calculation of the potential distribution in Multiple Ion Slit Lens
C. MONGINI-TAMAGNINI - to be issued

(2) Numerical calculation of the Potential Distribution in Ion Slit Lens System I
A.J.H. BOERBOOM - Z. Naturforschung 14a, 809-816 (1959)

(3) Numerical calculation of the Potential Distribution in Ion Slit Lens System II
A.J.H. BOERBOOM - Z. Naturforschung 15a, 244-252 (1960)

(4) Computer program for the solution of Elliptic Partial Differential Equations
J.S. HORNSBY - CERN 63-7 (1963)

(5) A Pulsed High-Current Proton Source and Associated Focusing System
A. YOKOSAWA - Proc. Intern. Conf. High Energy Accelerators BNL Upton, USA (1961) 385

(6) TRION - A program to calculate trajectories of charged particles in electrostatic fields
G. GAGGERO - to be issued

(7) Contour Map Subroutines
P. MOINIL, J. PIRE - report EUR 2241 f (1965)

(8) Design of an Ion Selector for Ion Implantation in Semiconductors
L. STANCHI - Nucl. Instr. and Meth. 73 (1969) 313

(9) Some calculations concerning the focalization properties of an ion analyzer
G. GAGGERO - EUR report to be issued

(10) The development of magnetic ion sources for an electromagnetic isotope separator.
K.O. NIELSEN - Nucl. Instr. and Meth. 1 (1957) 289

(11) Proc. Intern. Symp. Vienna (1960)
O. SKILBREID and G. SIDENIUS

(12) Preparation and some properties of conducting transparent glass
R. GOMER - Rev. Sci. Instr. 24 (1953) 993

(13) Fluorescent screens for observation of heavy ion beams
D.A. HALL - Rev. Sci. Instr. 36 (1965) 1512

FIGURES CAPTION

Fig. 1.1 - Schematic layout of the 100 KeV ion accelerator.

Fig. 1.2 - The 100 KeV ion implantation machine.

Fig. 1.3 - Simplified block diagram showing high voltage supply connections.

Fig. 2.1 - Equipotential distribution curves in the acceleration chamber of the preliminary system - Source potential: 10 KV; Einzel Lens potential: 6.5 KV.

Fig. 2.2 - Ion trajectories calculated for M = 84 amu, I = 12 μ A - Source potential: 6 KV; Einzel Lens potential: 4.6 KV.

Fig. 2.3 - Plots of the output radius of the beam cross-section vs current having the angle of aperture of the magnet as a parameter. The curves for smaller angles are derived by curves for 127° in which the original input radius is suitable enlarged. The three curves of every plot consider the same input radius r_o.

Fig. 2.4 - Ion trajectories in the constant field tube at 20 KV decelerating potential.
M = 84 amu, I = 12 μ A, energy of the ions at the tube input: 50 KeV.

Fig. 3.1 - Block diagram of the ion source cooling circuit.

Fig. 3.2 - Electrical layout of the source power supply.

Fig. 4.1 - Acceleration chamber of the preliminary system.

Fig. 4.2 - Acceleration chamber end plate showing the Einzel Lens and, on a rotating sector, the Faraday cup and the fluorescent screen.

Fig. 4.3 - Ion beam diameter vs Einzel Lens potential at different values of the acceleration gap.

Fig. 4.4 - Ion beam diameters VS distance from the source outlet. Calculated diameters are reported in one case for comparison.

Fig. 4.5 - Distribution of an Argon ion beam along the X and Y axis taken by a hand operated beam scanner. The beam cross-section as determined by a square rules fluorescent screen is reported.

Fig. 4.6 - X-Y scan of an Argon ion beam not homogeneous and with elliptic cross-section.

Fig. 4.7 - Definitive acceleration chamber and lens system.

Fig. 4.8 - Simplified schematic of the comparison between H.V. output and reference voltage for obtaining regulation (V_1 supply).

Fig. 4.9 - Simplified schematic of the balance between H.V. and reference voltage for obtaining regulation (V_2 supply). Note the different position of the switches in the case of positive or negative voltage.

Fig. 4.10 - Block diagram of V_1 supply.

Fig. 4.11 - Set up of V_1 and V_2 supplies.

Fig. 5.1 - Simplified layout of the analyzing magnet.

Fig. 5.2 - Block diagram of the current regulated magnet supply.

Fig. 5.3 - Magnetic induction vs current at the center of the iron gap.

Fig. 5.4 - Magnetic induction values in the saturating and not saturating region taken in a cross-section of the gap at the center of the magnet.

Fig. 5.5 - Mass spectrum of Xe (from M= 130 to M = 132) as displayed with the beam scanner.

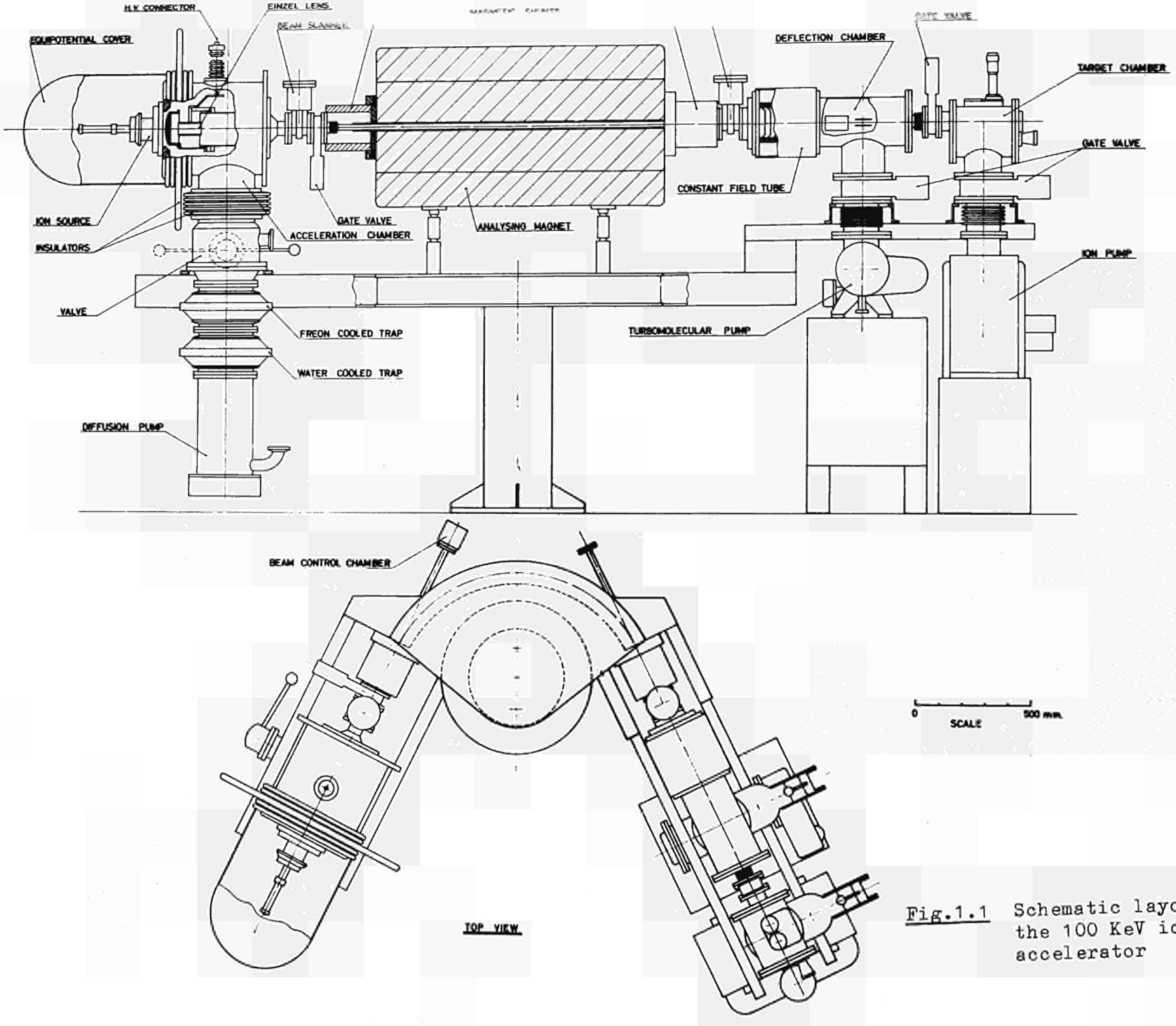

Fig.1.1 Schematic layout of the 100 KeV ion accelerator

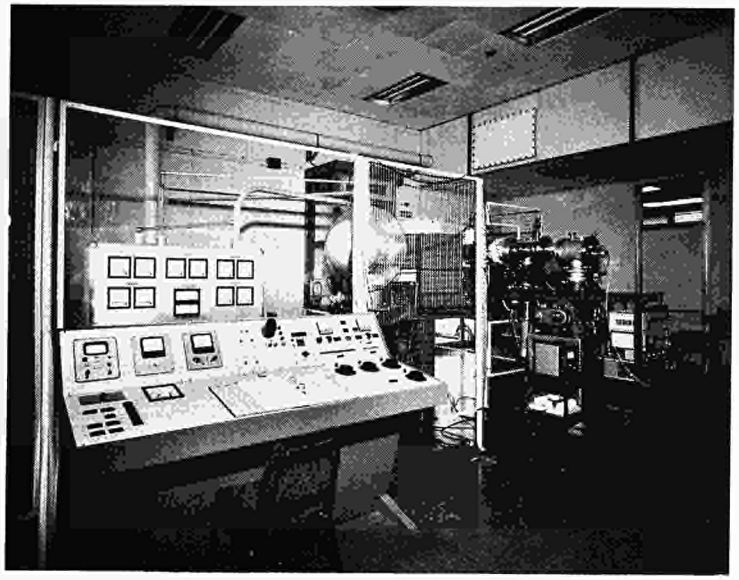

Fig. 1.2 The 100 KeV ion implantation machine

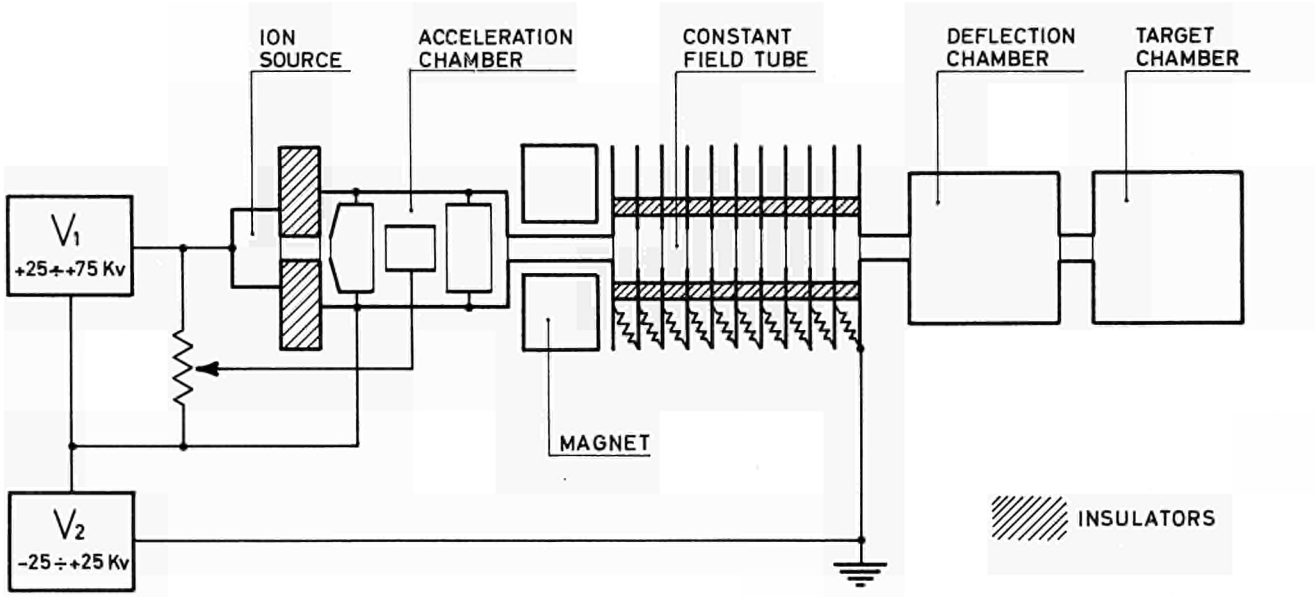

Fig. 1.3 Simplified block diagram showing high voltage supply connections

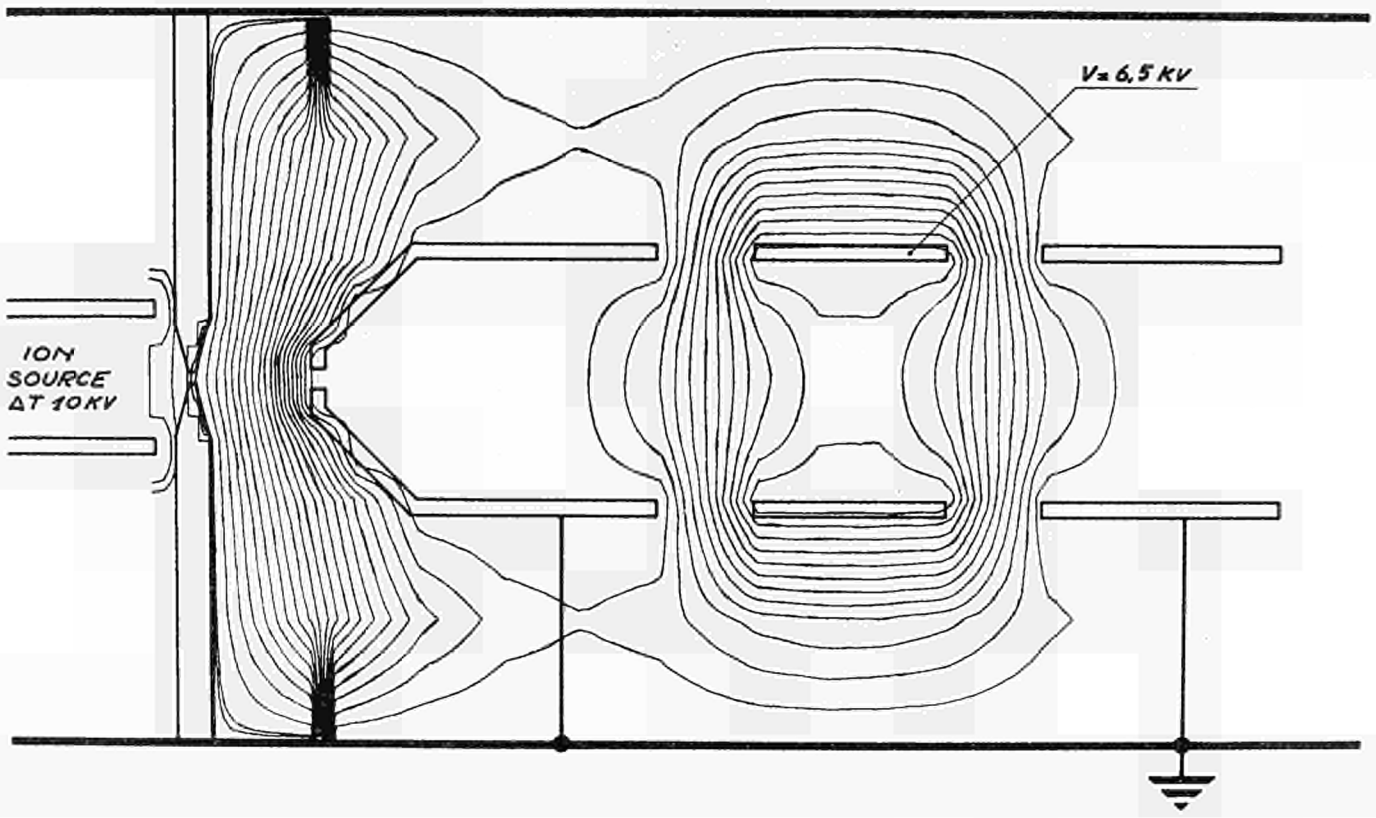

Fig. 2.1 Equipotential distribution curves in the acceleration chamber of the preliminary system - Source potential: 10 KV; Einzel Lens potential: 6.5 KV

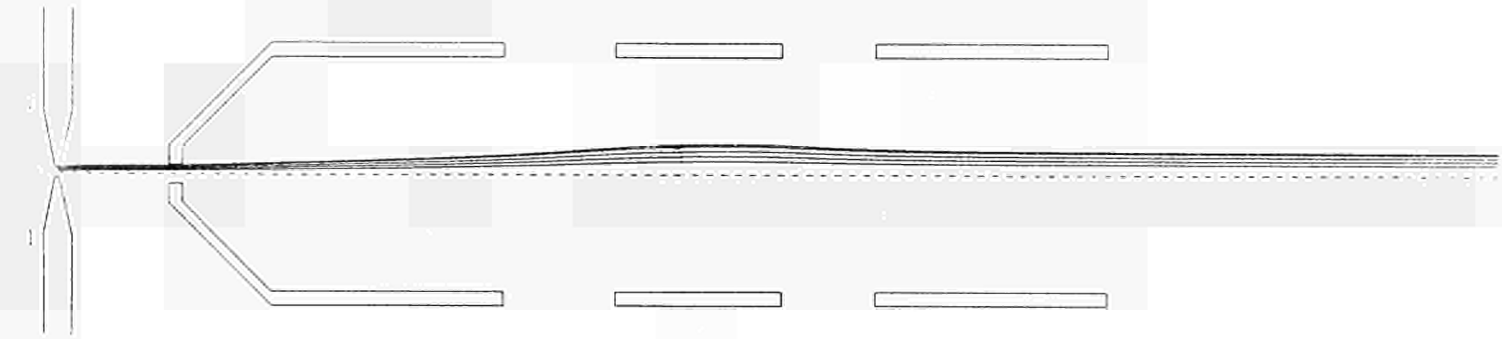

Fig. 2.2 Ion trajectories calculated for M = 84 amu, I = 12 μ A - Source potential: 6 KV; Einzel Lens potential: 4.6 KV

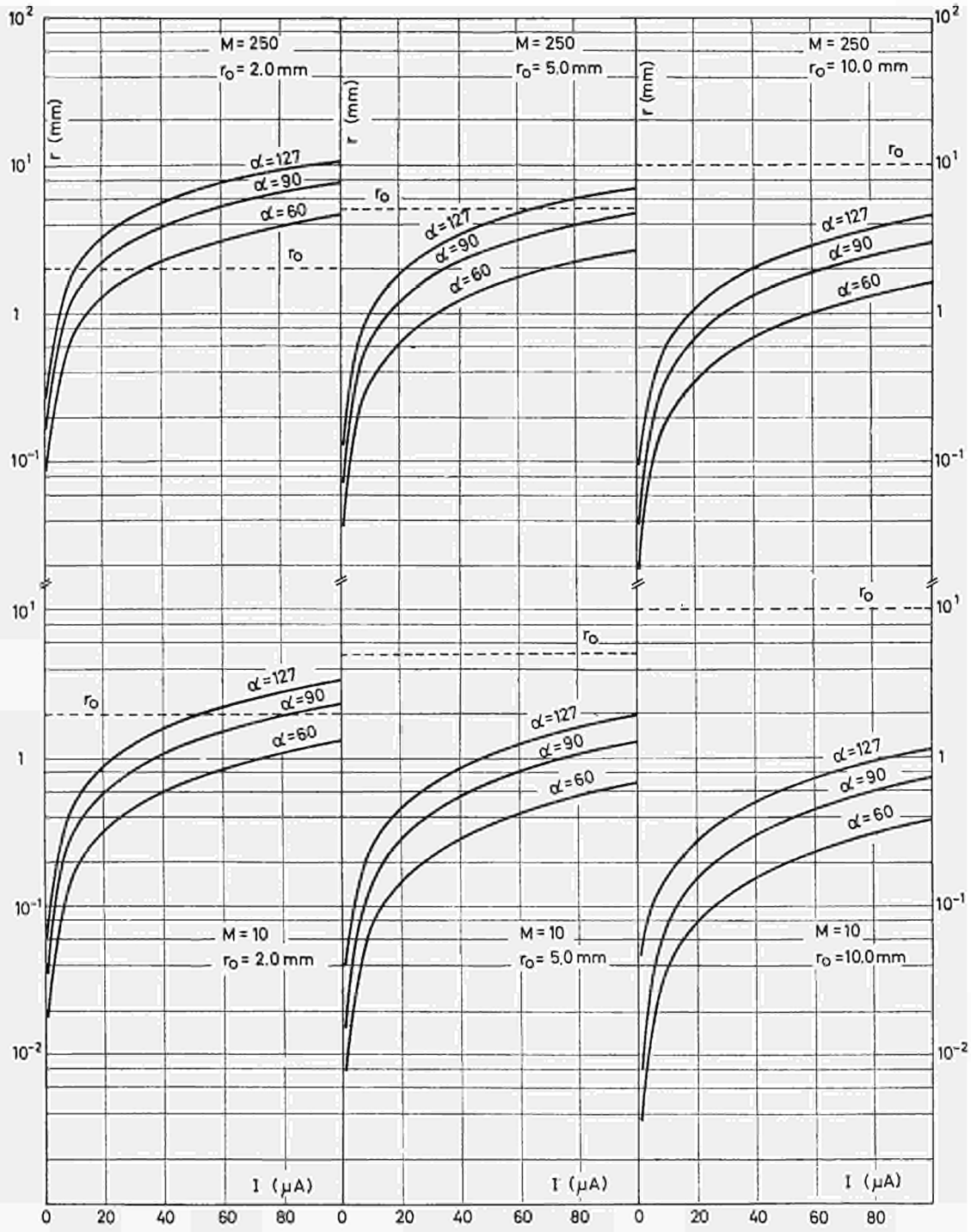

Fig. 2.3 Plots of the output radius of the beam cross-section vs current having the angle of aperture of the magnet as a parameter. The curves for smaller angles are derived by curves for 127 ° in which the original input radius is suitable enlarged. The three curves of every plot consider the same input radius r_o.

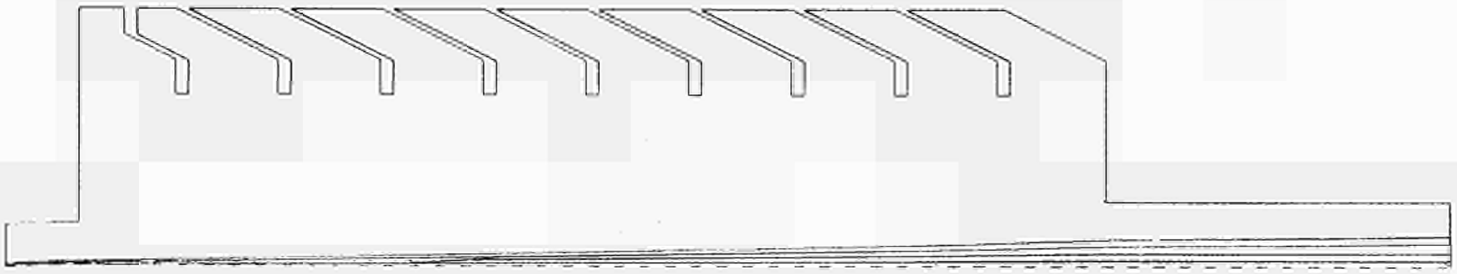

Fig. 2.4 Ion trajectories in the constant field tube at 20 KV decelerating potential
M = 84 amu, I = 12 μA, energy of the ions at the tube input: 50 KeV

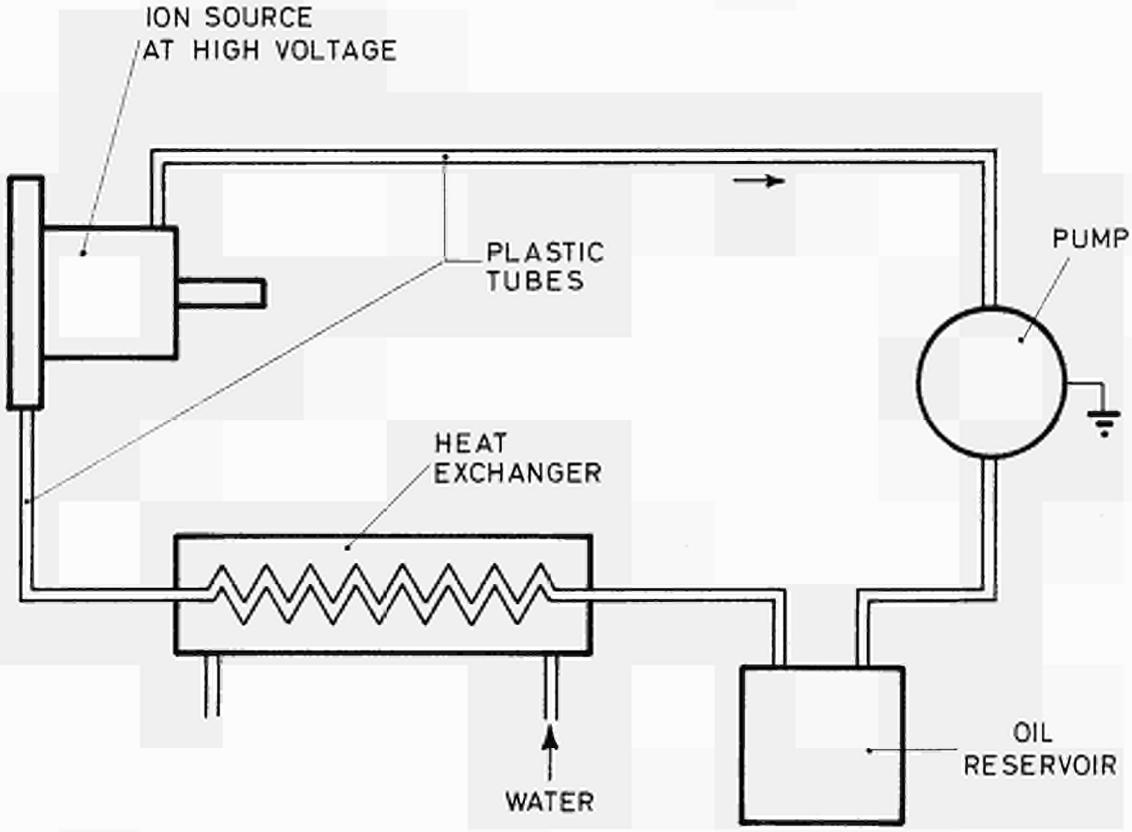

Fig. 3.1 Block diagram of the ion source cooling circuit

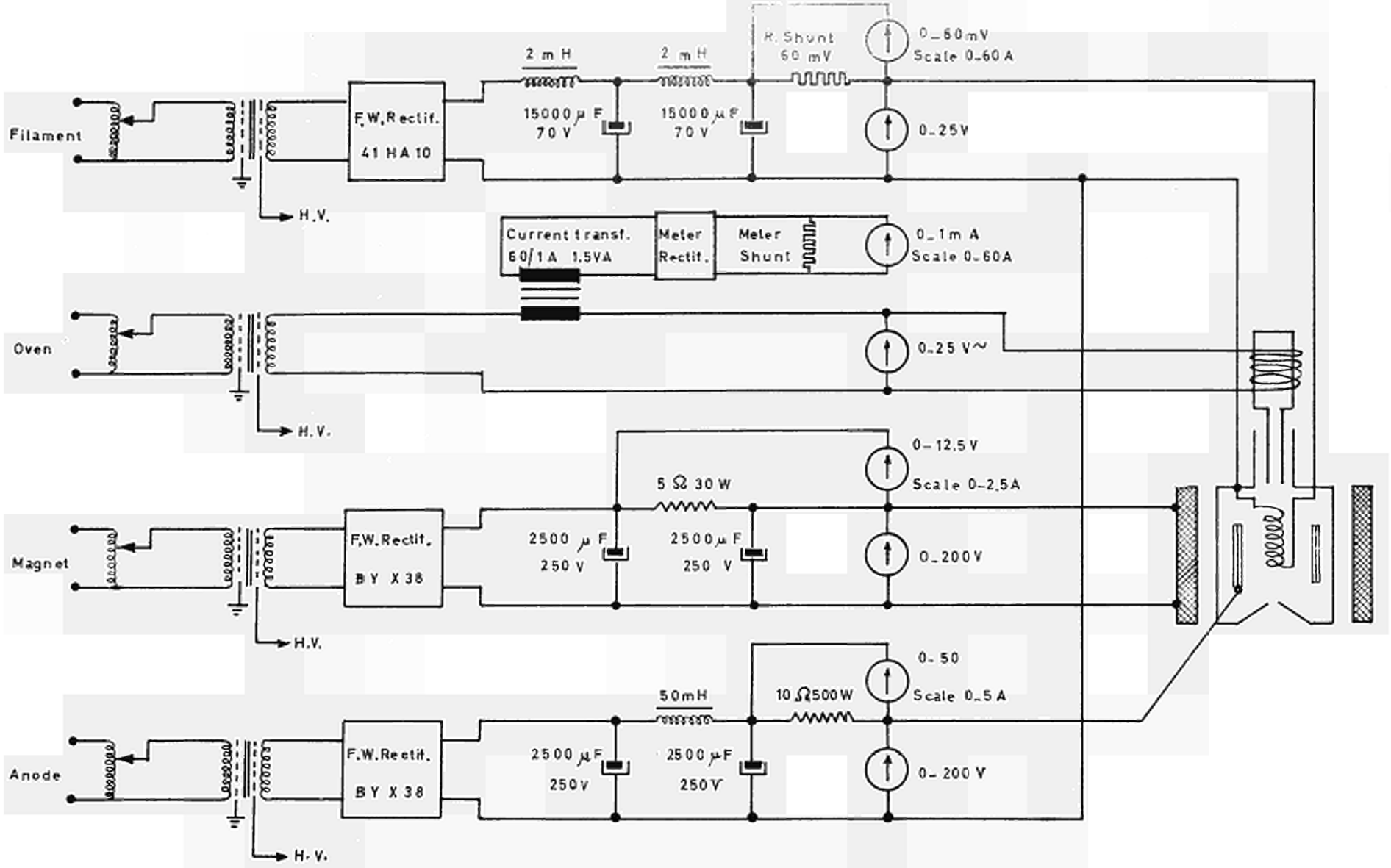

Fig. 3.2 ION SOURCE POWER SUPPLY

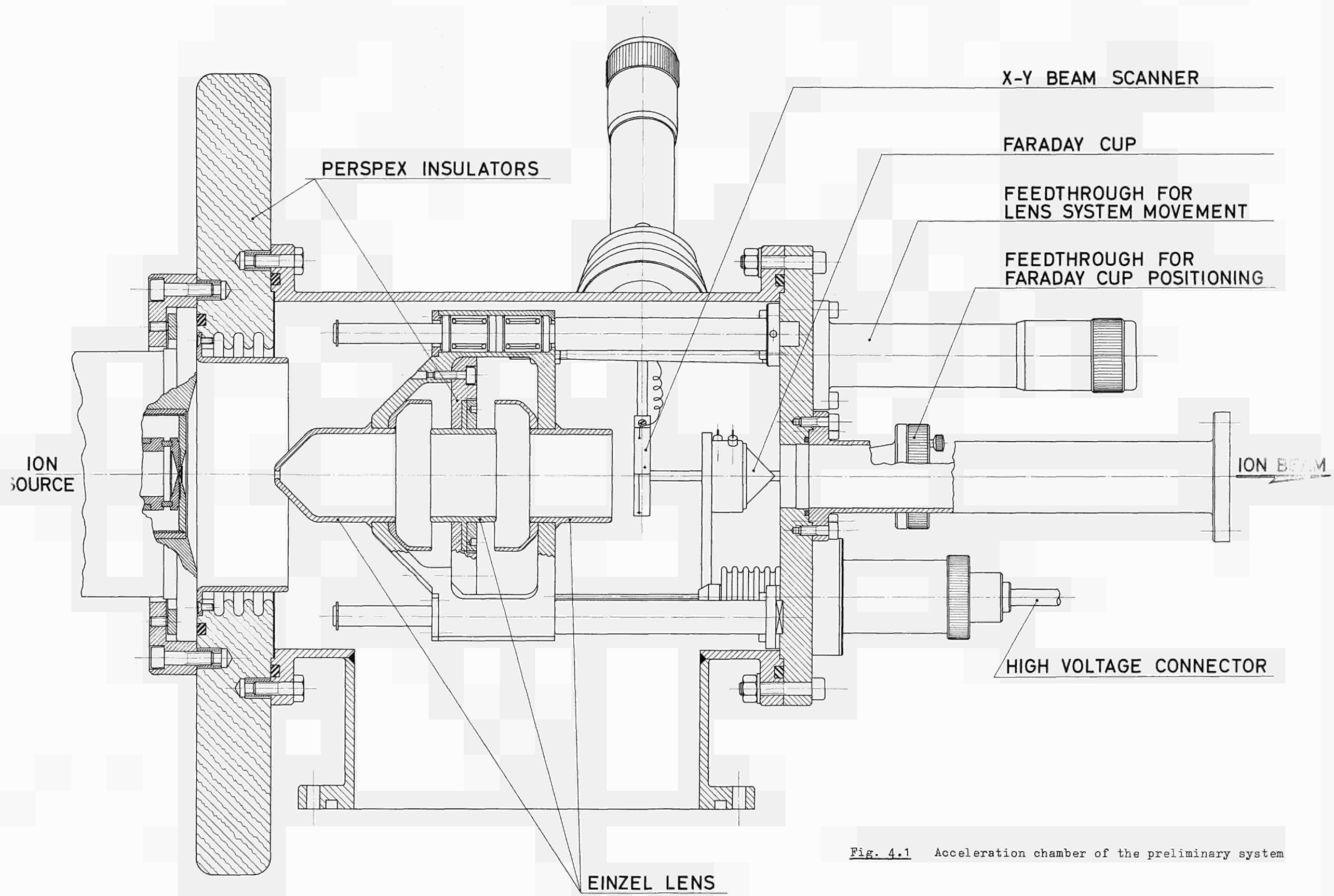

Fig. 4.1 Acceleration chamber of the preliminary system

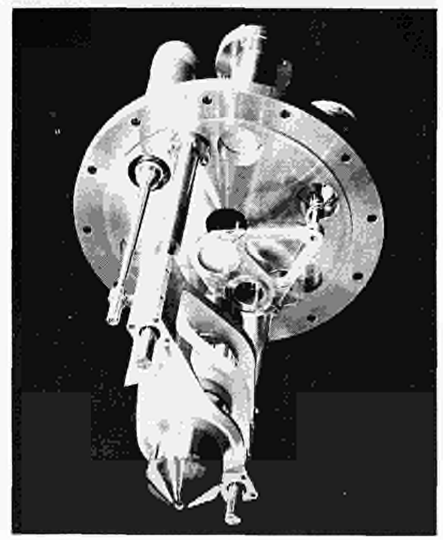

Fig. 4.2 Acceleration chamber end plate showing the Einzel Lends and, on a rotating sector, the Faraday cup and the fluorescent screen

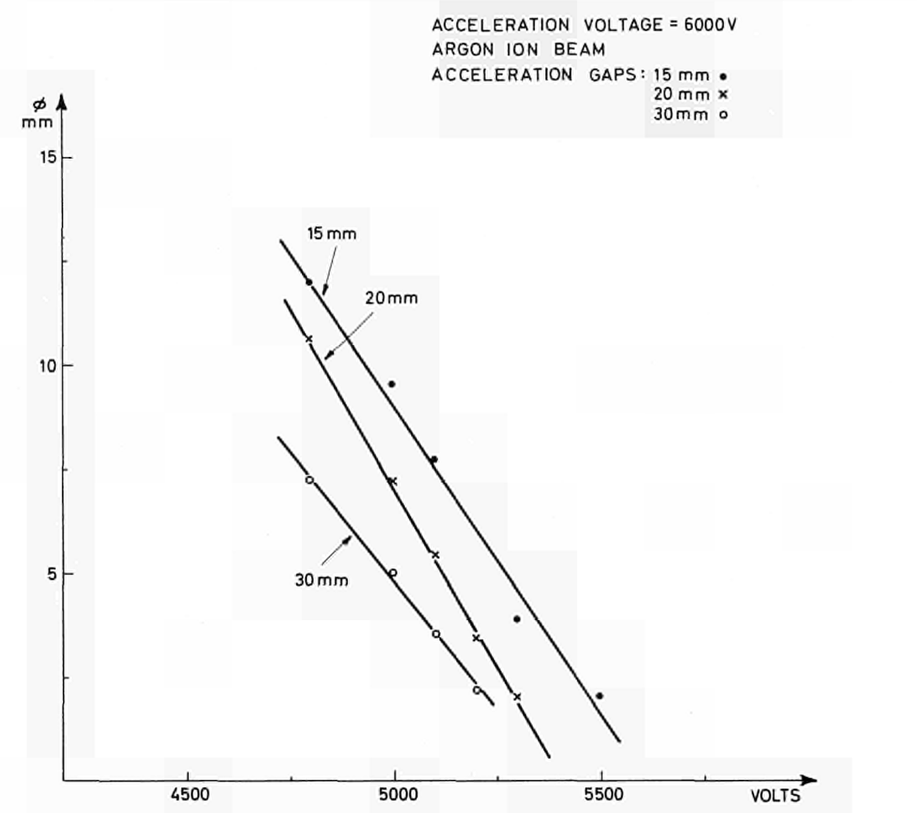

Fig. 4.3 Ion beam diameter vs Einzel Lens potential at different values of the acceleration gap

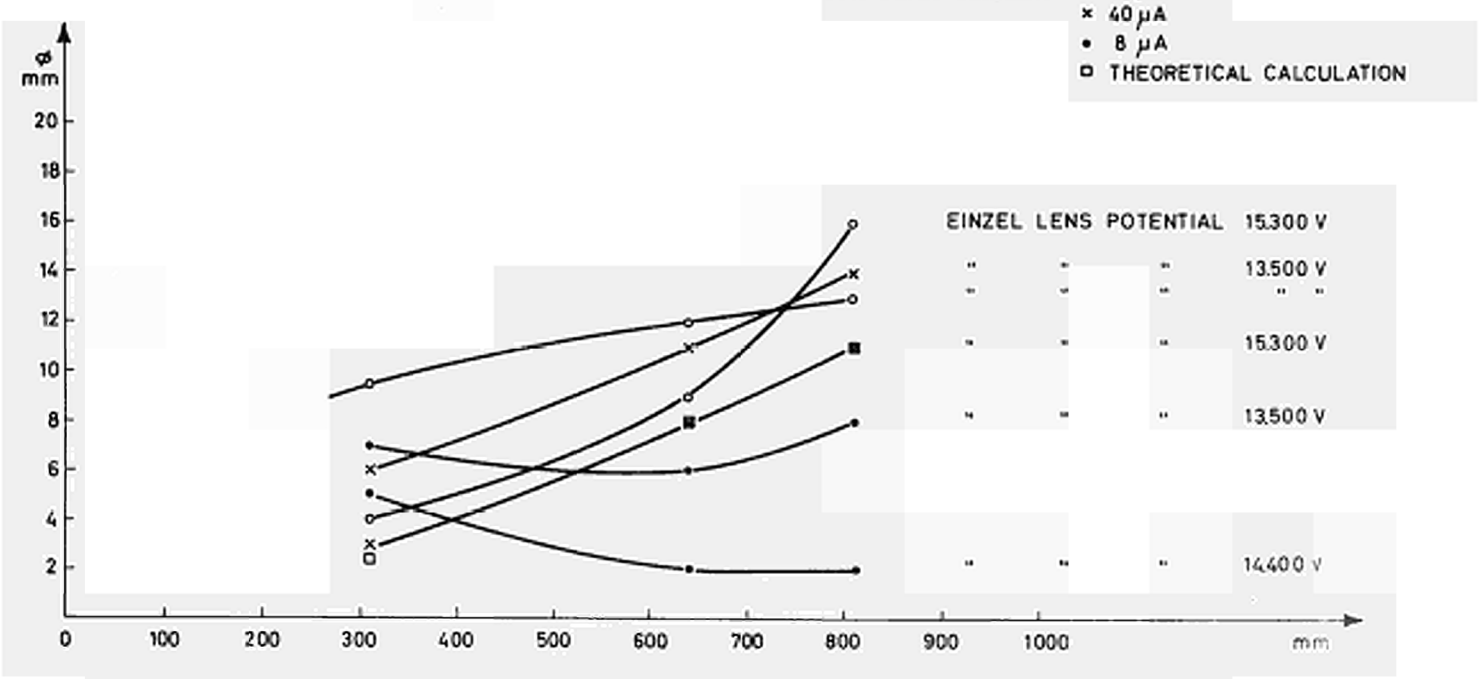

Fig. 4.4 Ion beam diameters Vs distance from the source outlet. Calculated diameters are reported in one case for comparison

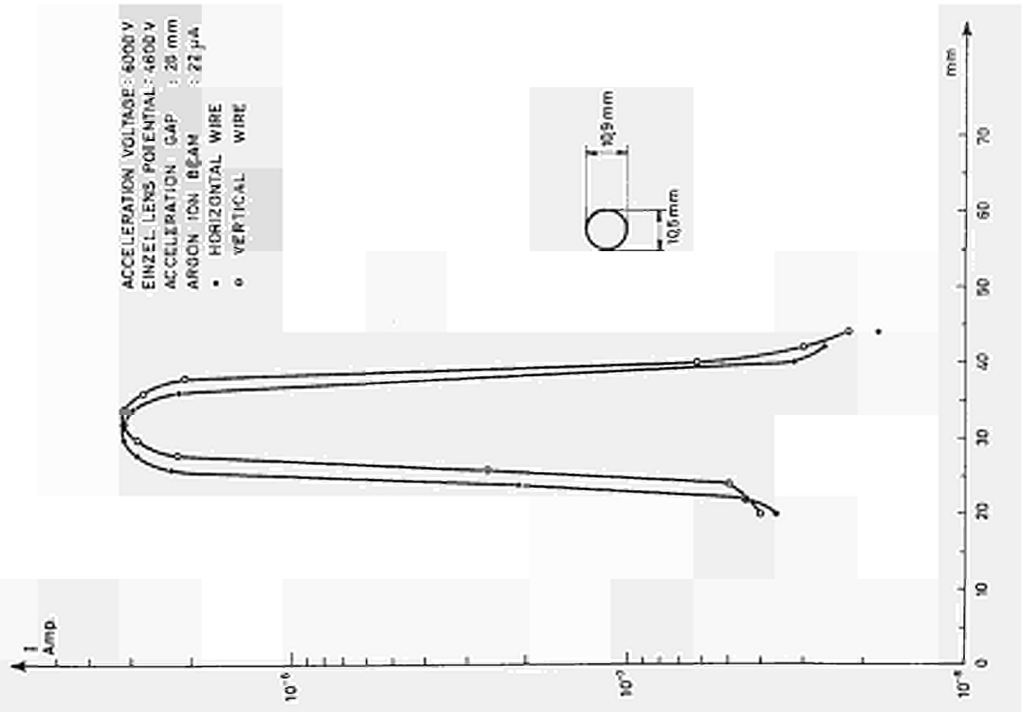

Fig. 4.5 Distribution of an Argon ion beam along the X and Y axis taken by a hand operated beam scanner. The beam cross-section as determined by a square rules fluorescent screen is reported

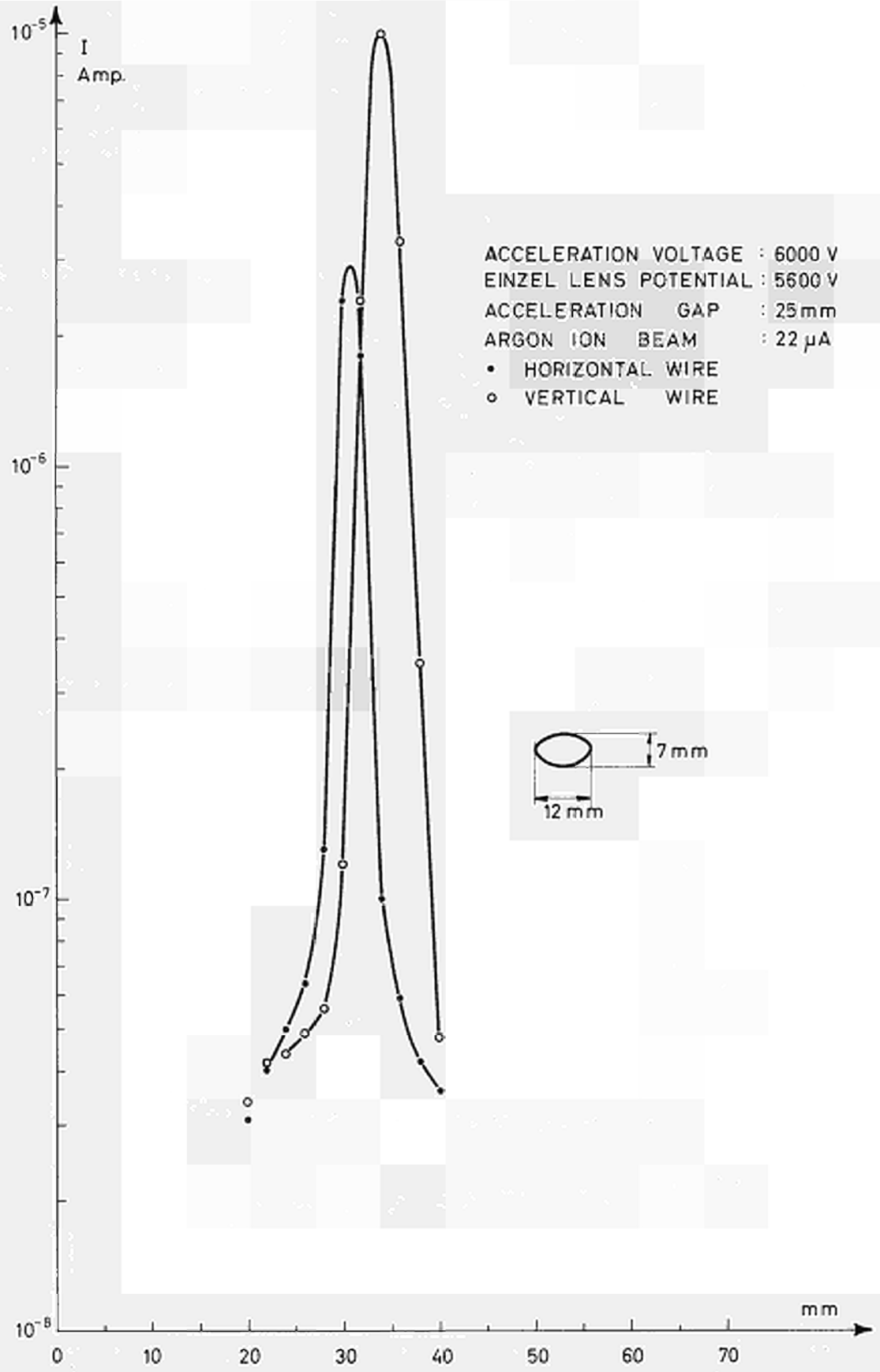

Fig. 4.6 X-Y scan of an Argon ion beam not homogeneous and with elliptic gross-section

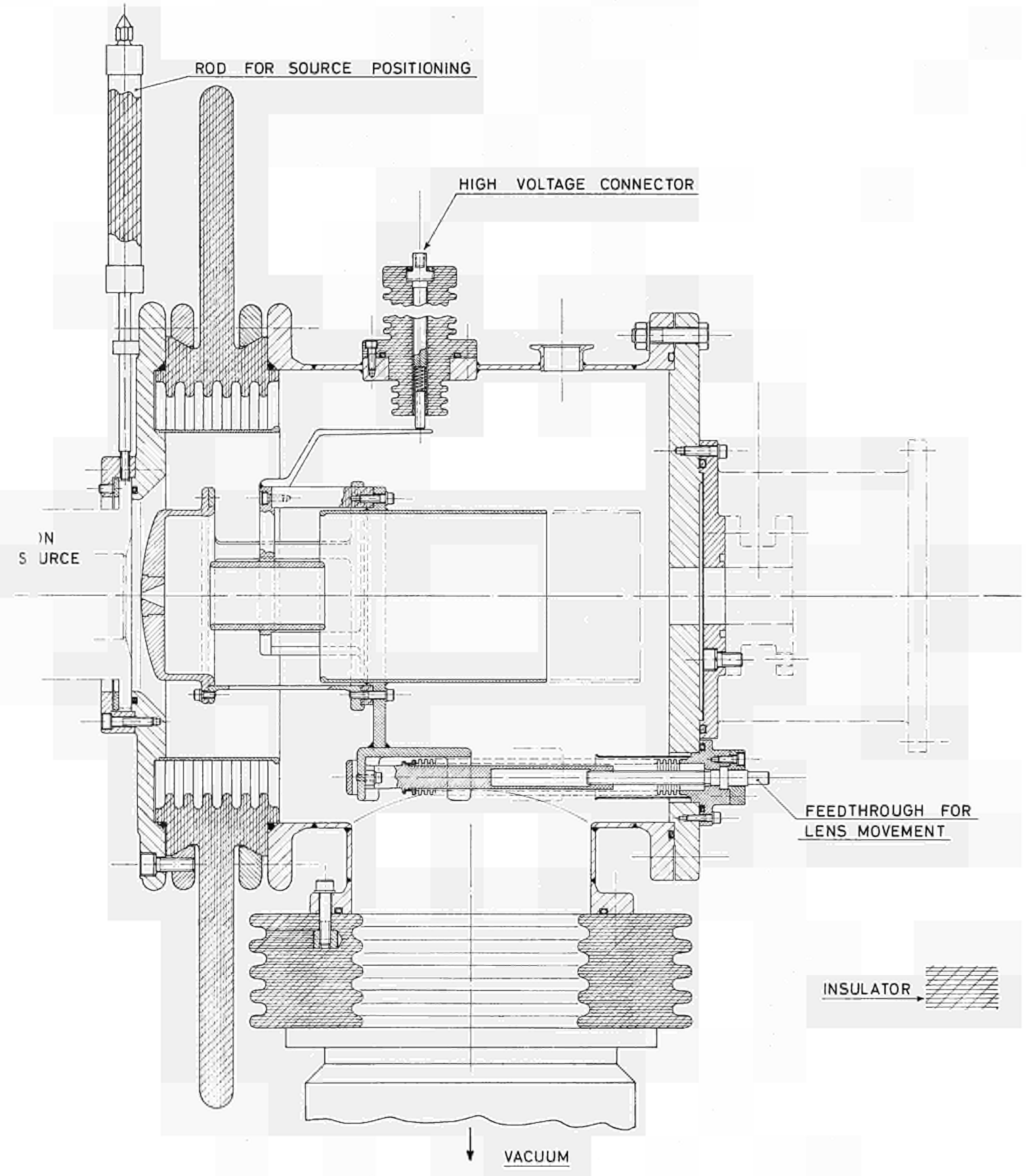

Fig. 4.7 Definitive acceleration chamber and lens system

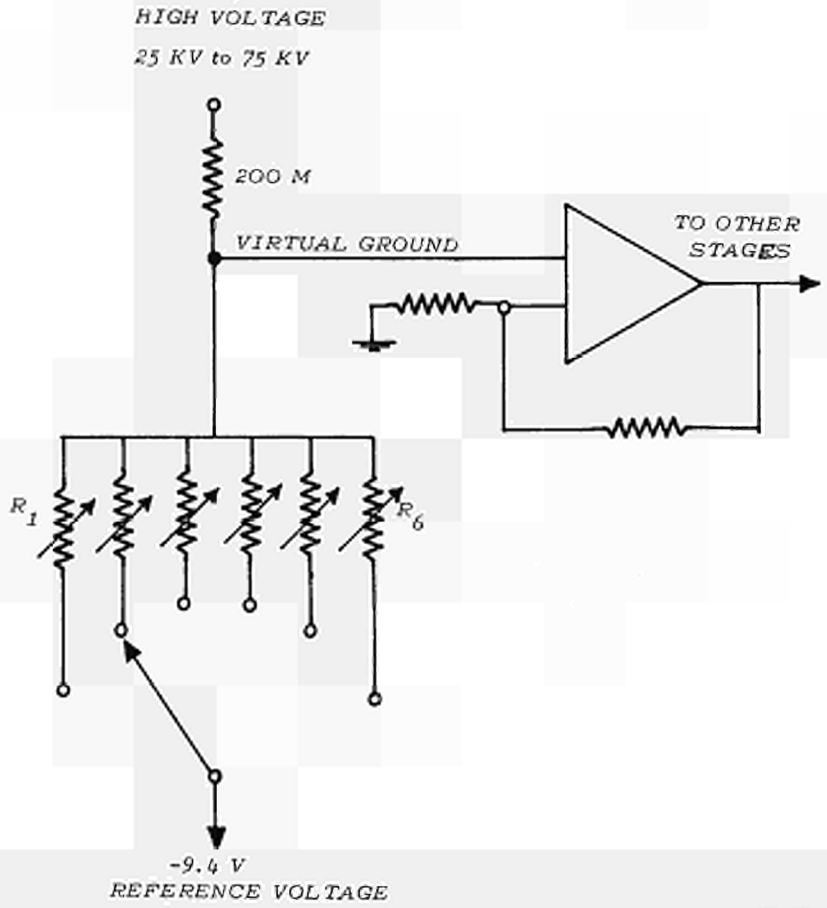

Fig. 4.8 Simplified schematic of the comparison between H.V. output and reference voltage for obtaining regulation (V_1 supply)

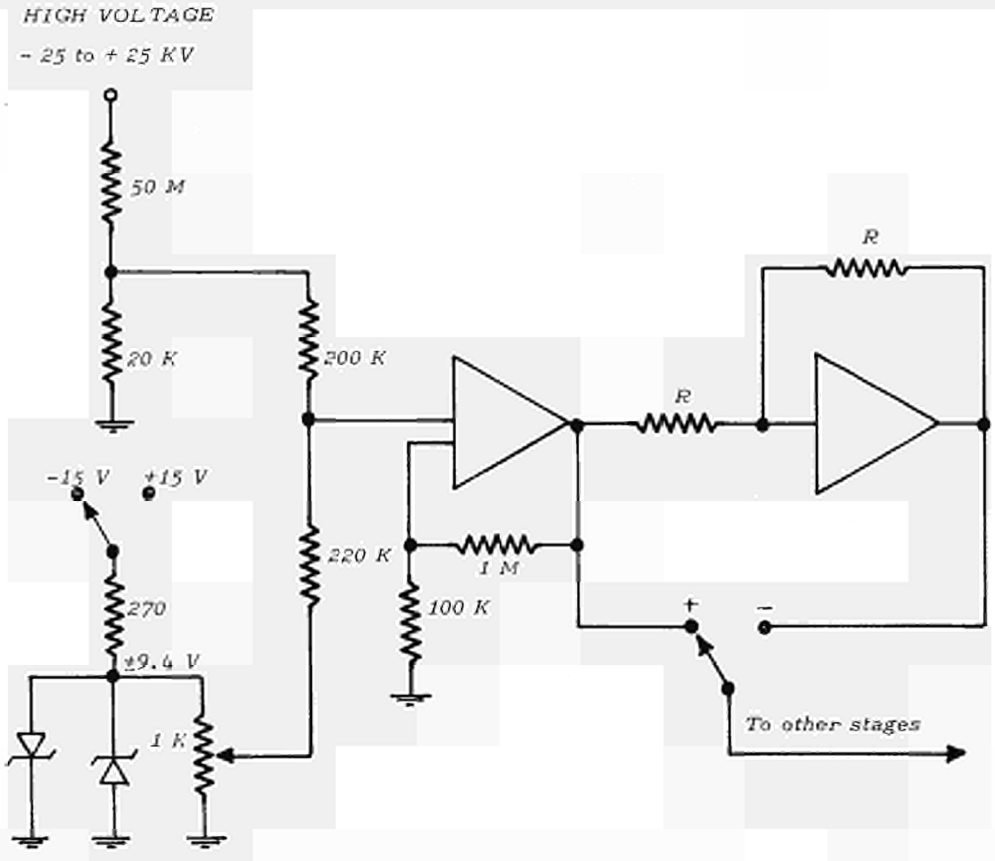

Fig. 4.9 Simplified schematic of the balance between H.V. and reference voltage for obtaining regulation (V_2 supply). Note the different position of the switches in the case of positive or negative voltage

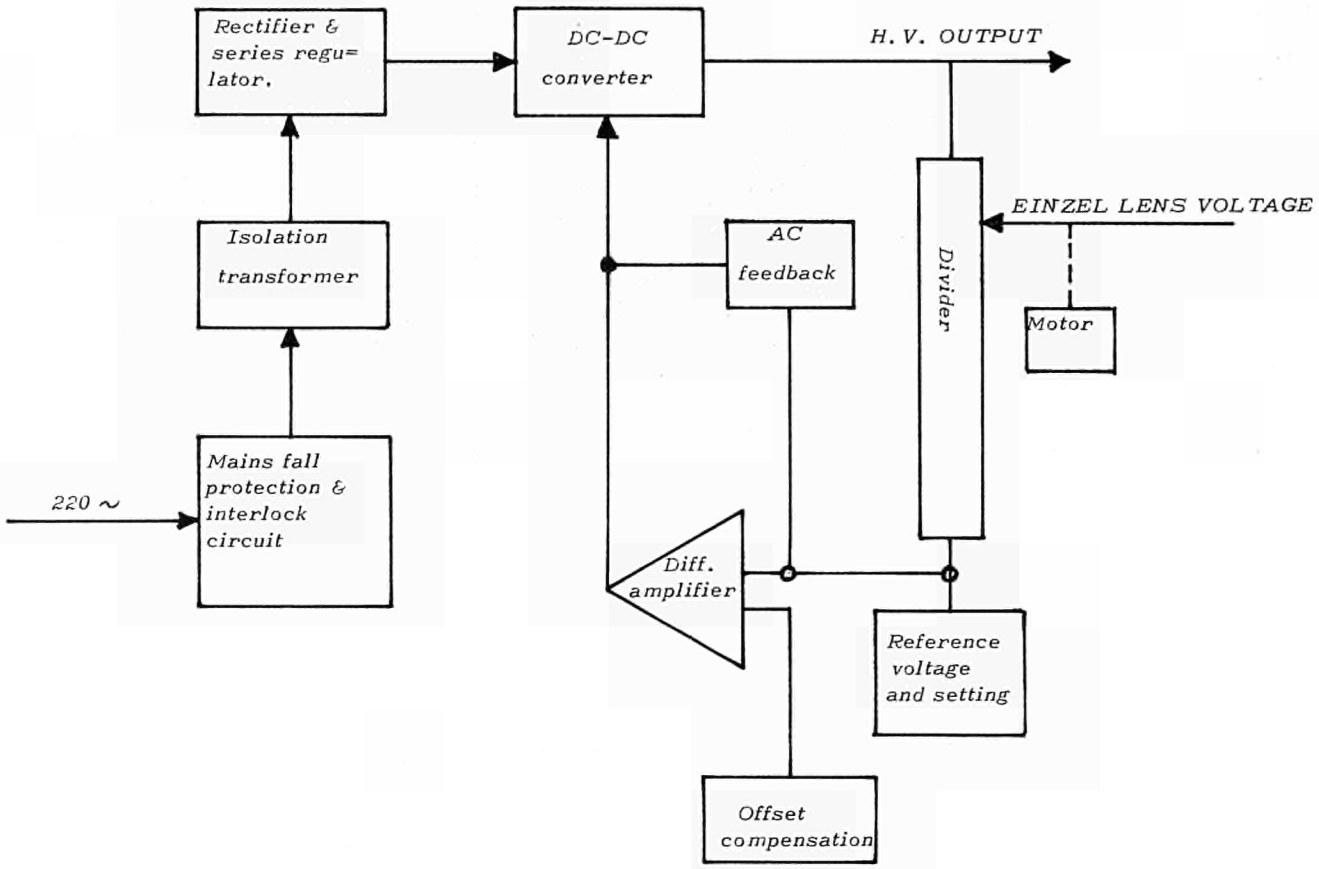

Fig. 4.10 Block diagram of V_1 supply

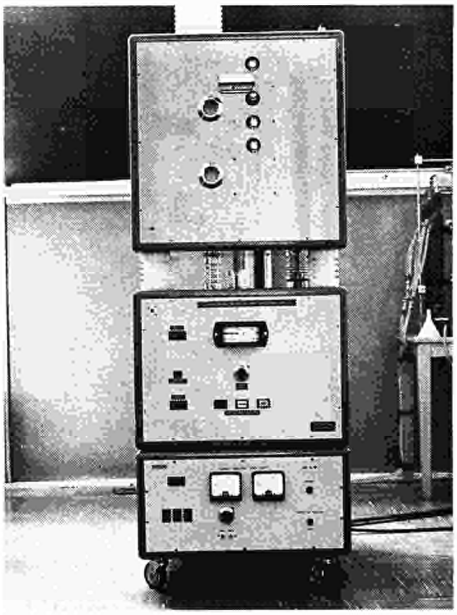

Fig. 4.11 Set up of V_1 and V_2 supplies

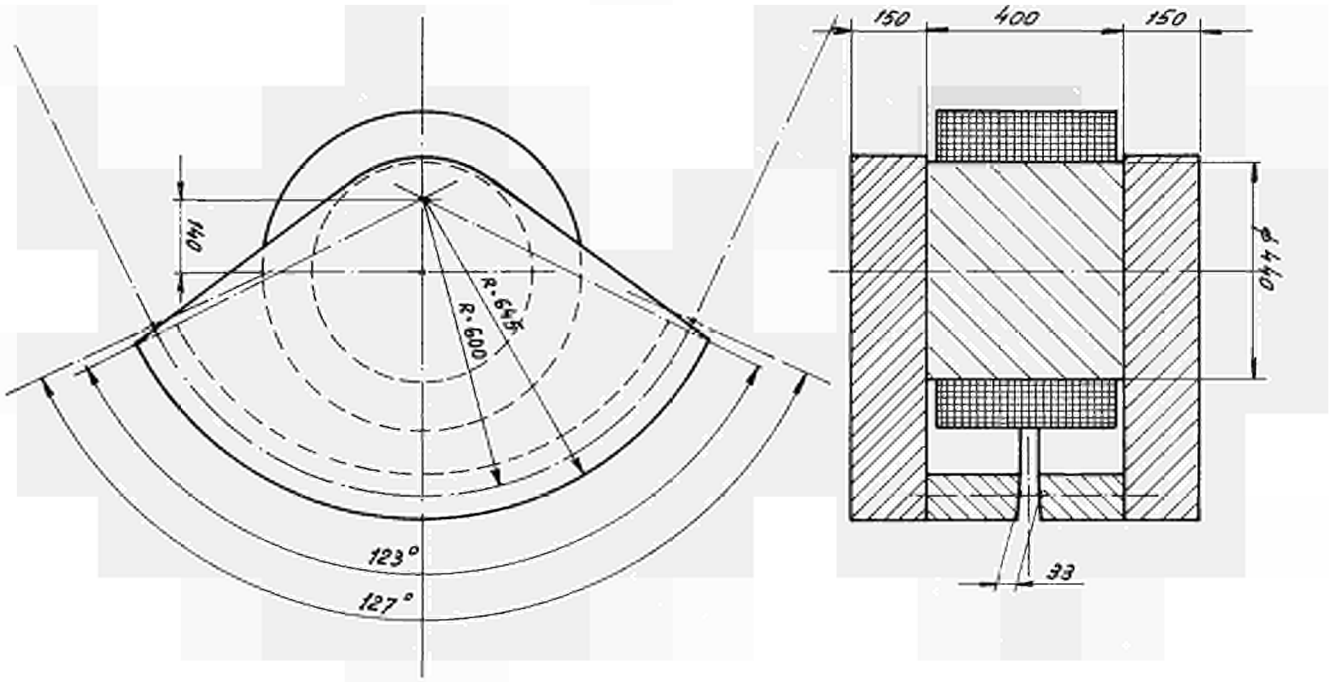

Fig. 5.1 Simplified layout of the analyzing magnet

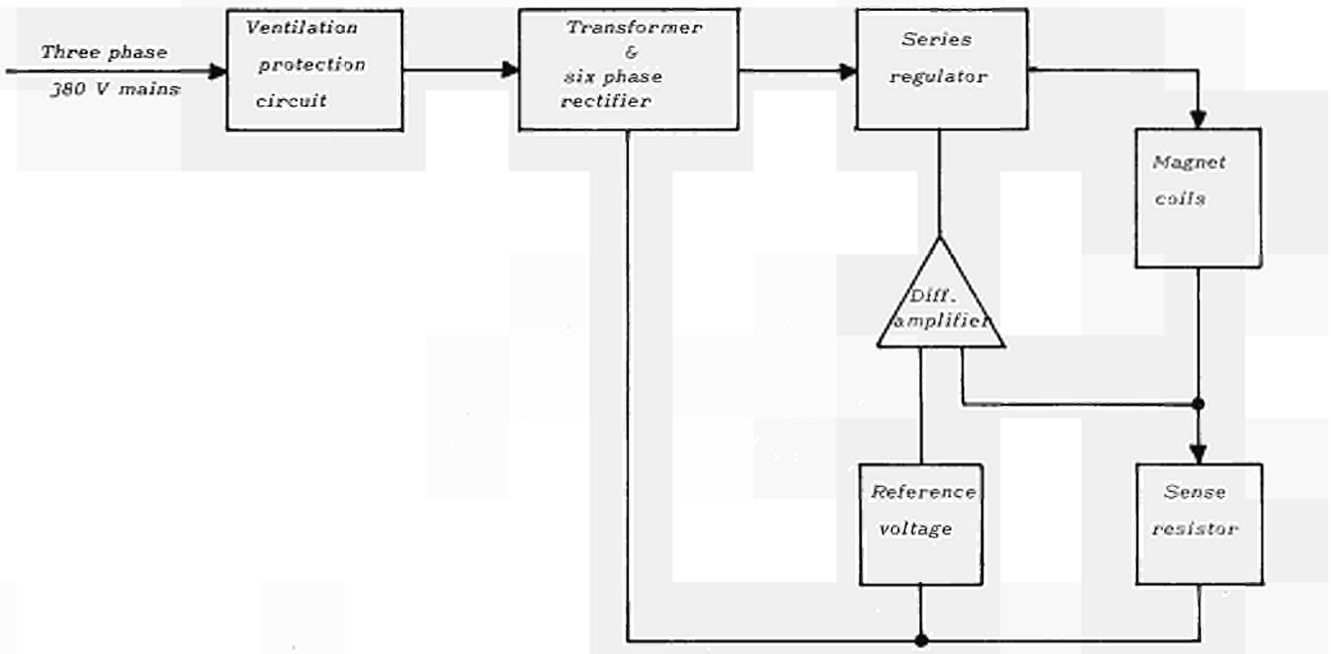

Fig. 5.2 Block diagram of the current regulated magnet supply

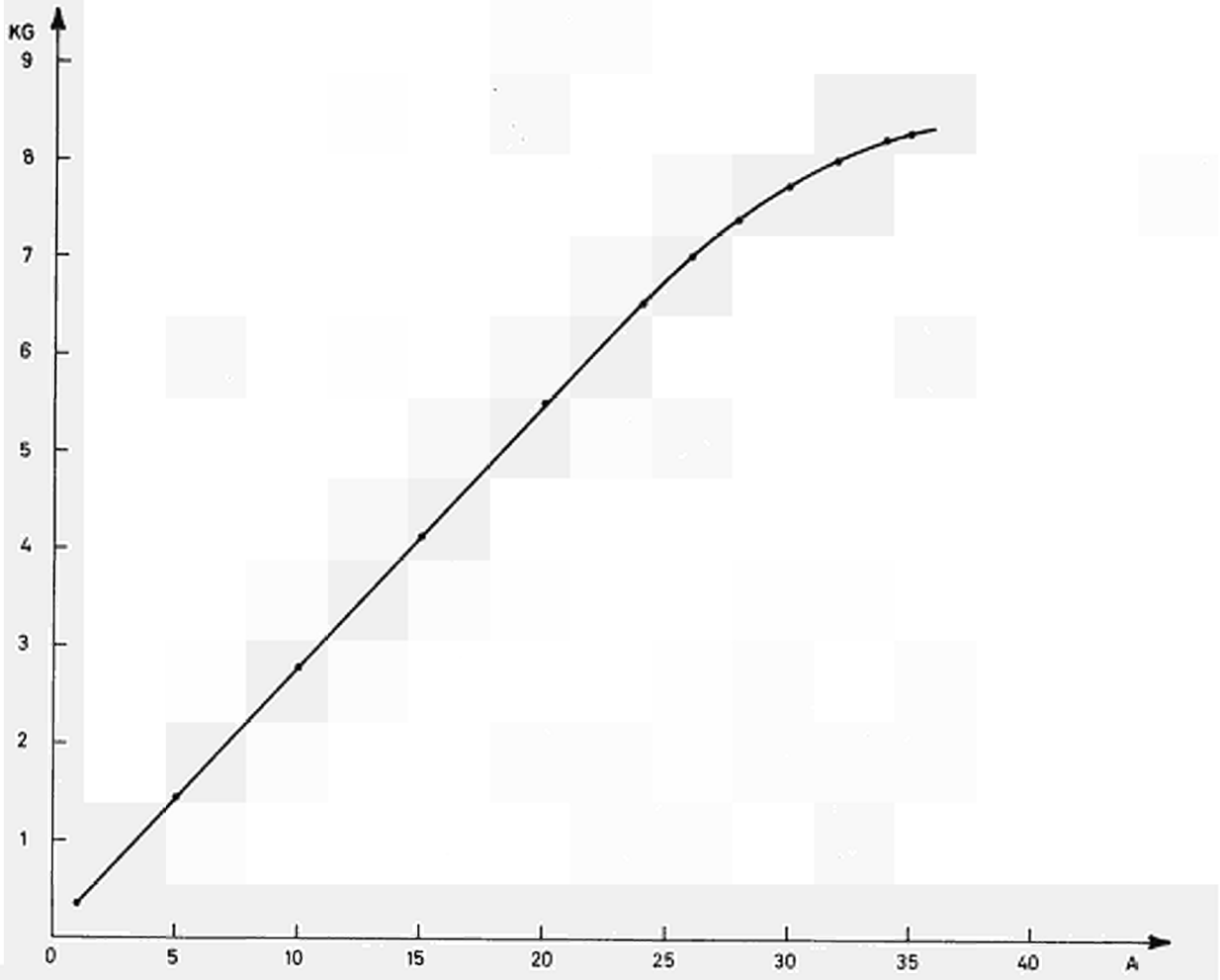

Fig. 5.3 Magnetic induction vs current at the center of the iron gap

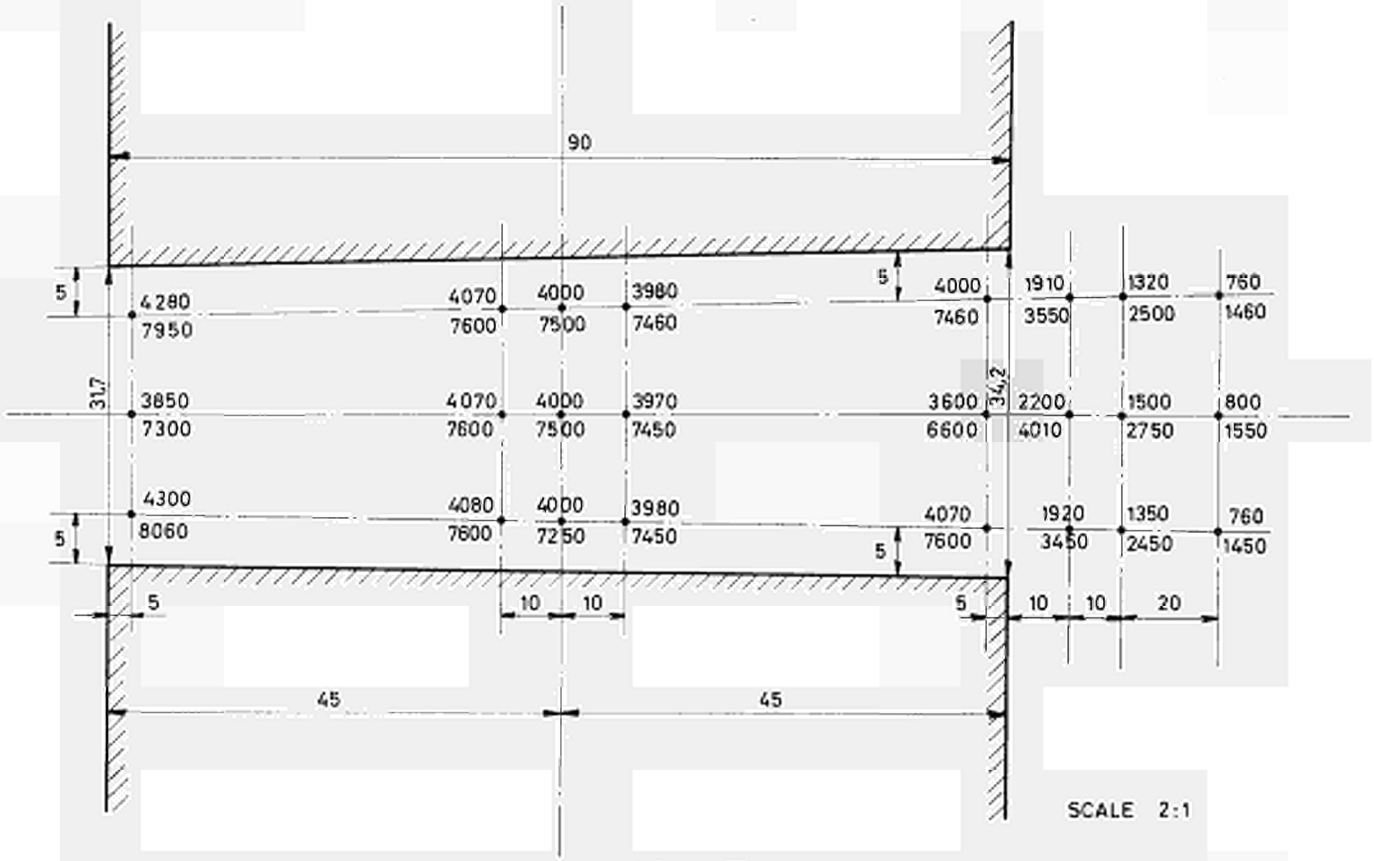

Fig. 5.4 Magnetic induction values in the saturating and not saturating region taken in a cross-section of the gap at the center of the magnet

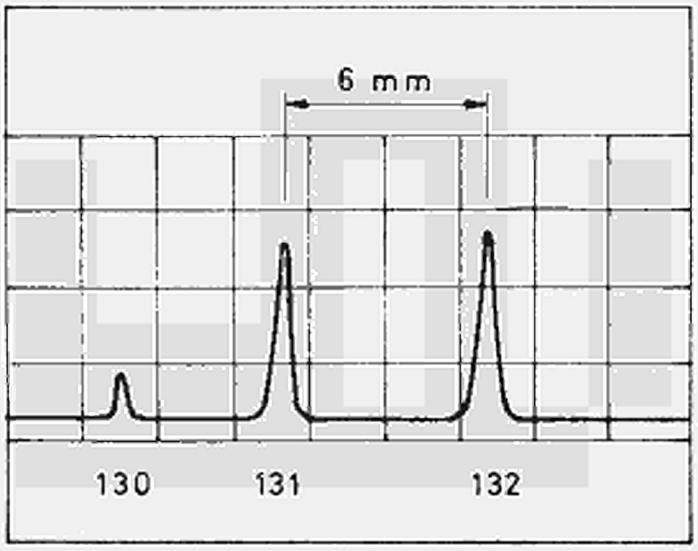

Fig. 5.5 Mass spectrum of Xe (from M= 130 toM = 132) as displayed with the beam scanner

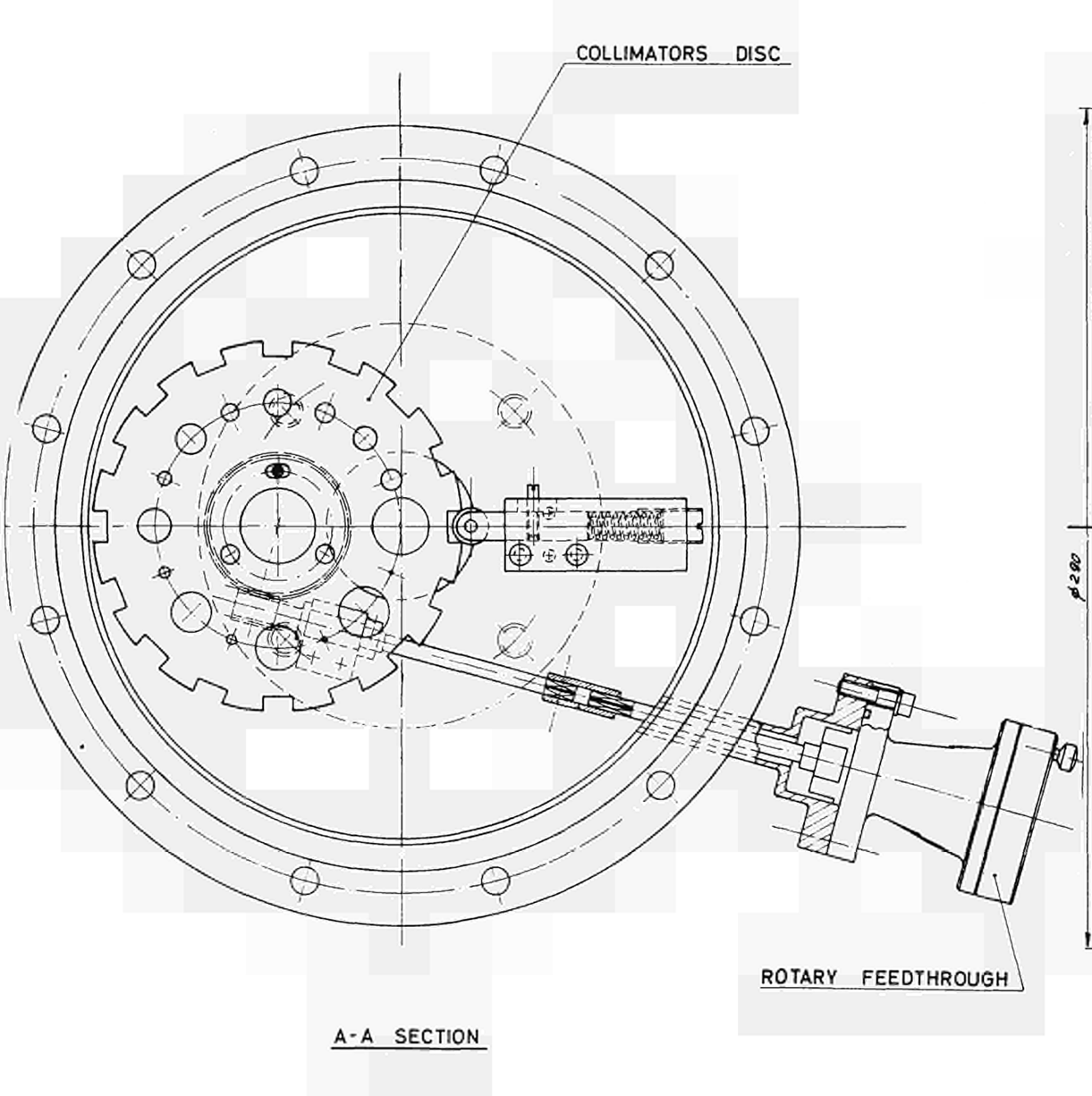

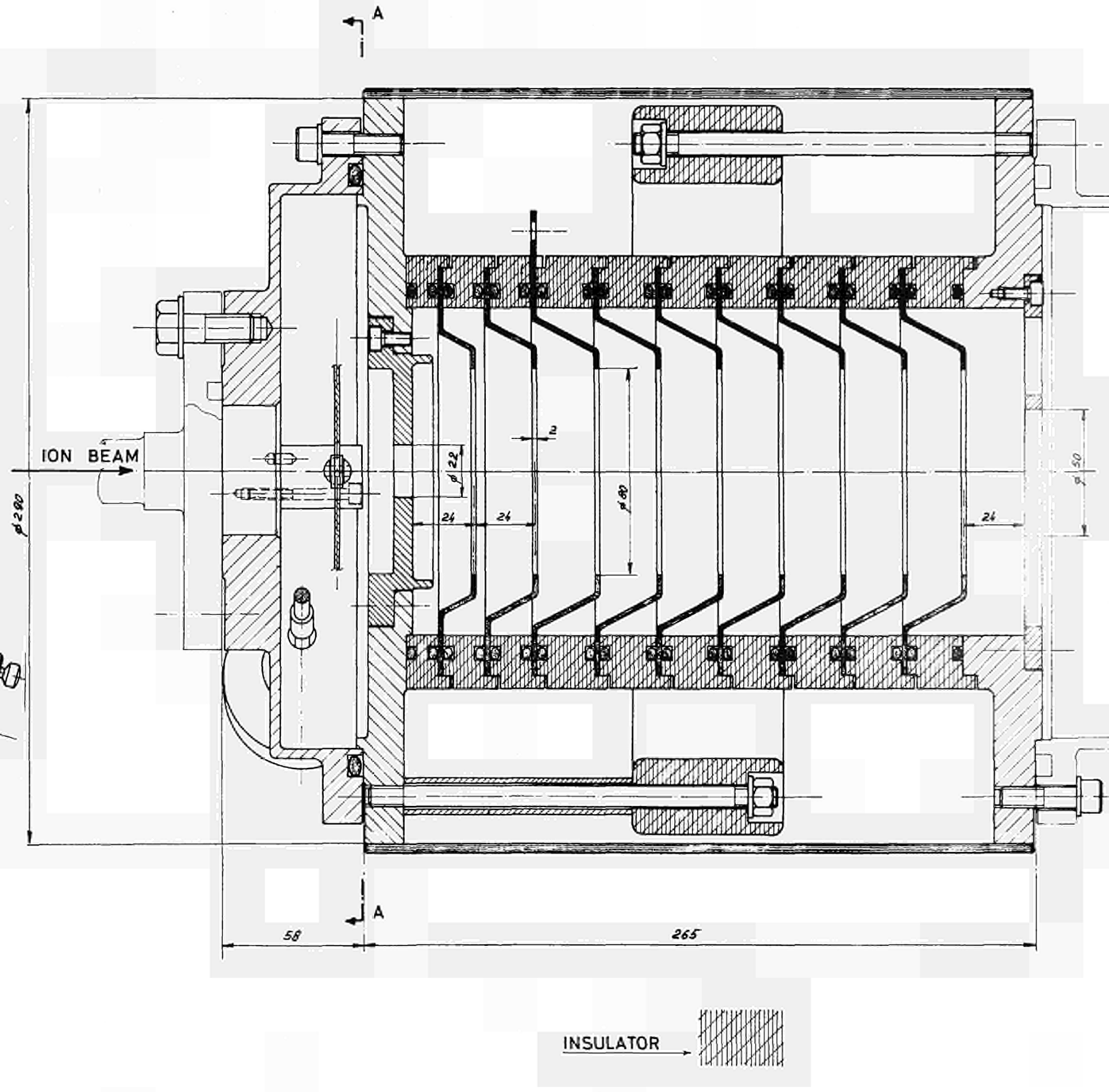

Fig. 6.1 Constant field tube

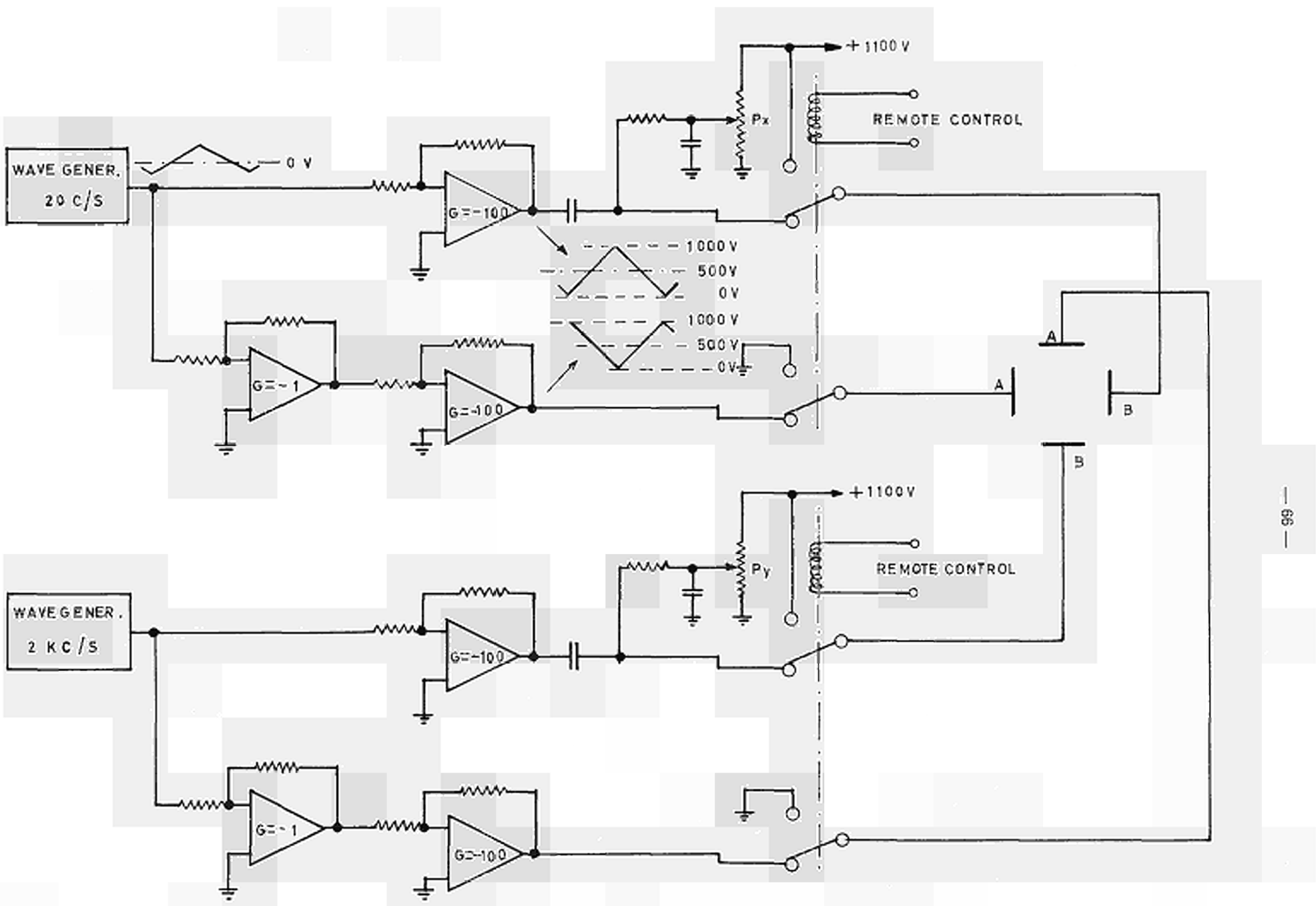

Fig. 7.1 BLOCK DIAGRAM OF THE BEAM SWEEPING SYSTEM

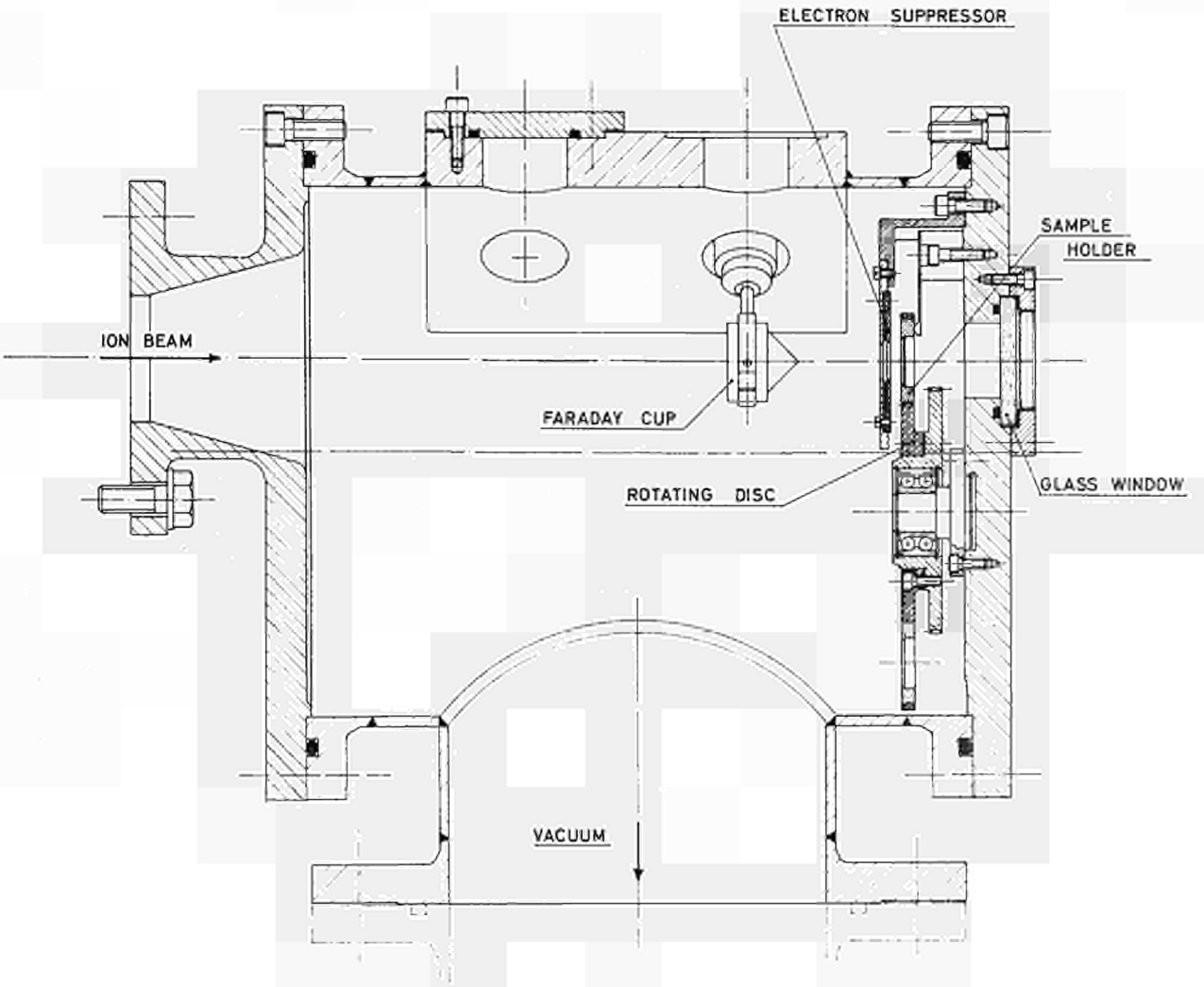

Fig. 8.1 Target chamber with plate for room temperature implantation

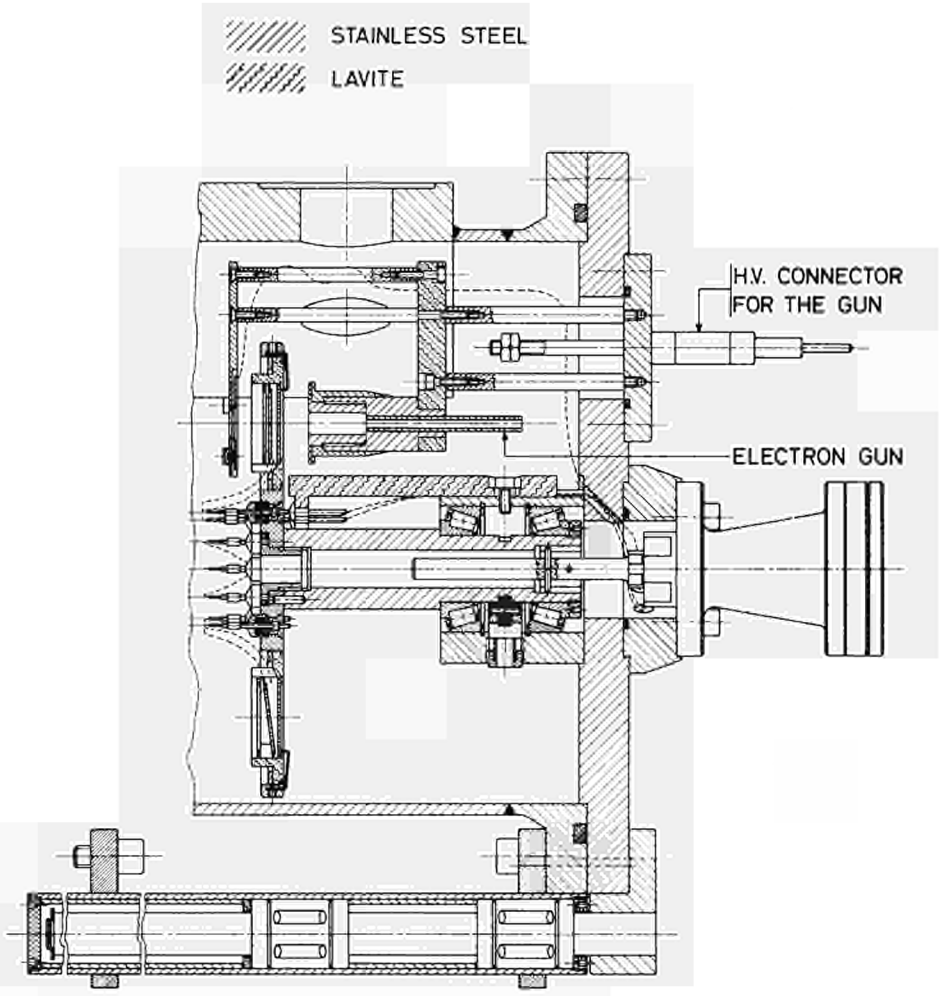

Fig. 8.2 Base plate for high temperature implantation

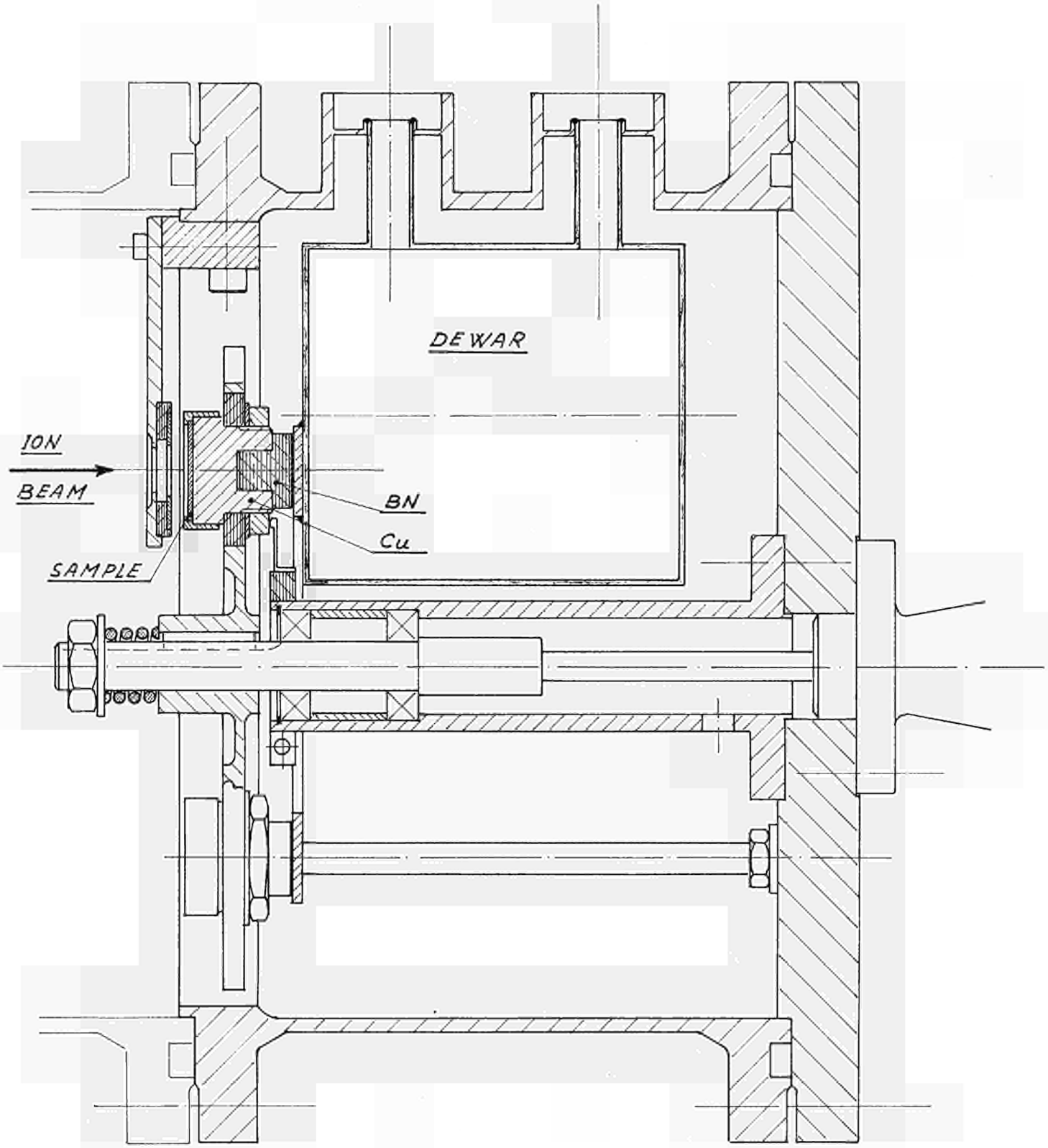

Fig. 8.3 Facility for low temperature implantation

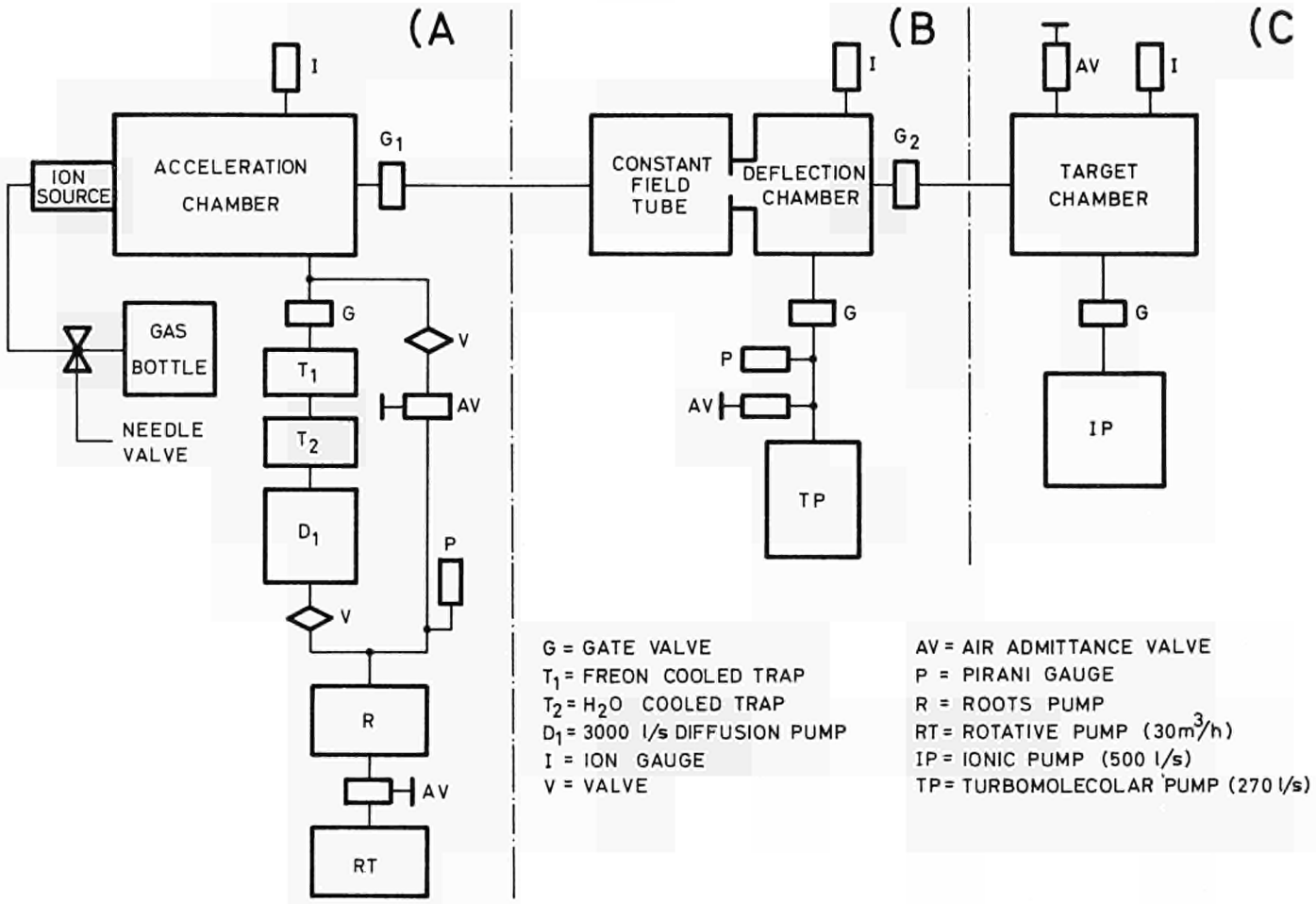

Fig. 9.1 Vacuum schematic

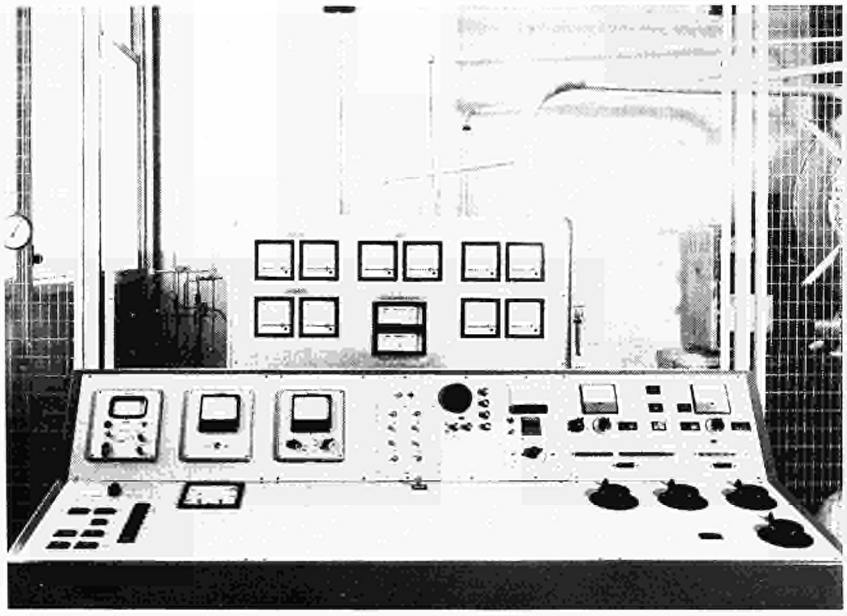

Fig. 10.1 Control desk

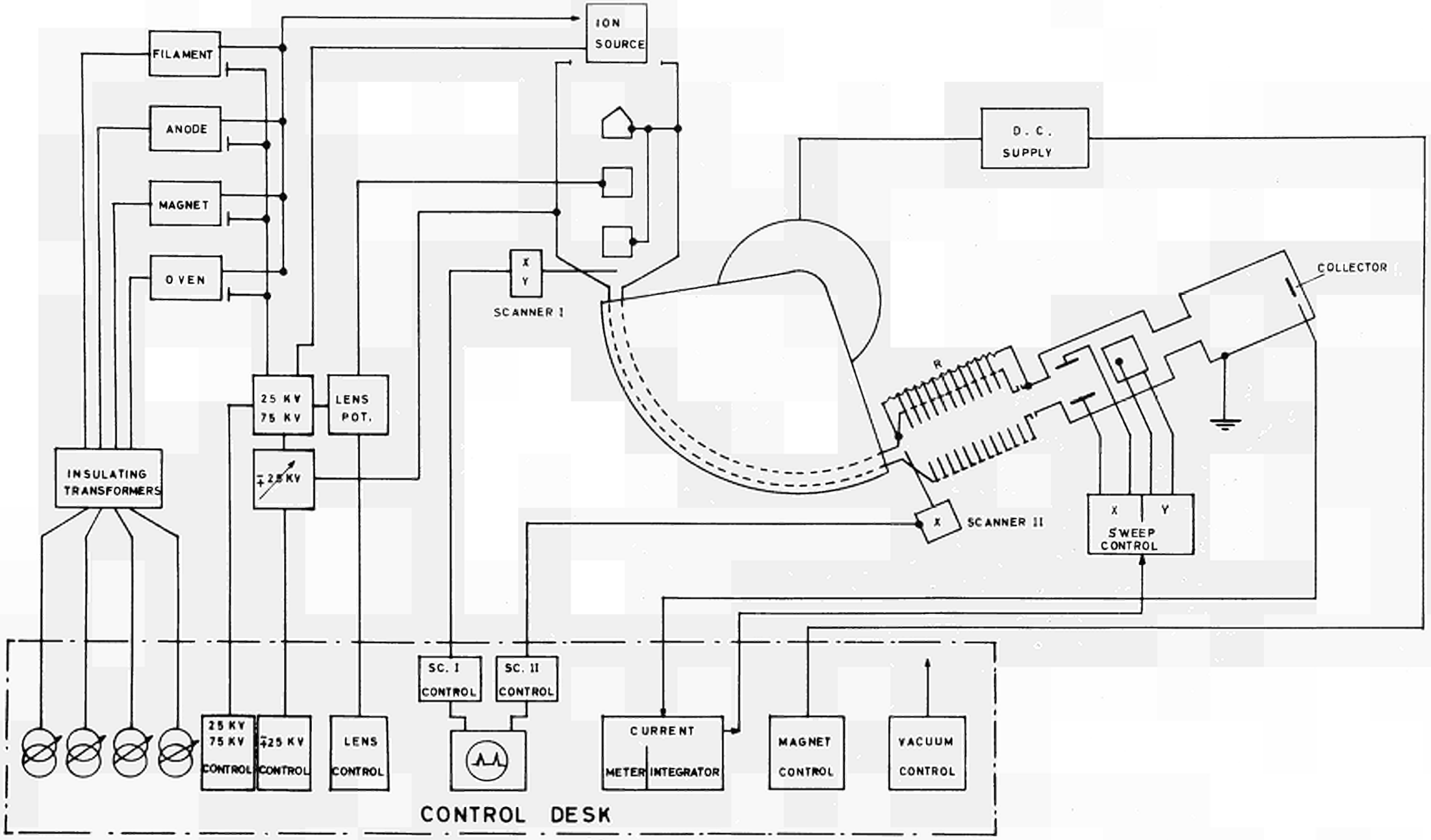

Fig. 10.2 SIMPLIFIED BLOCK DIAGRAM SHOWING THE VARIOUS SUPPLY AND CONTROL UNITS

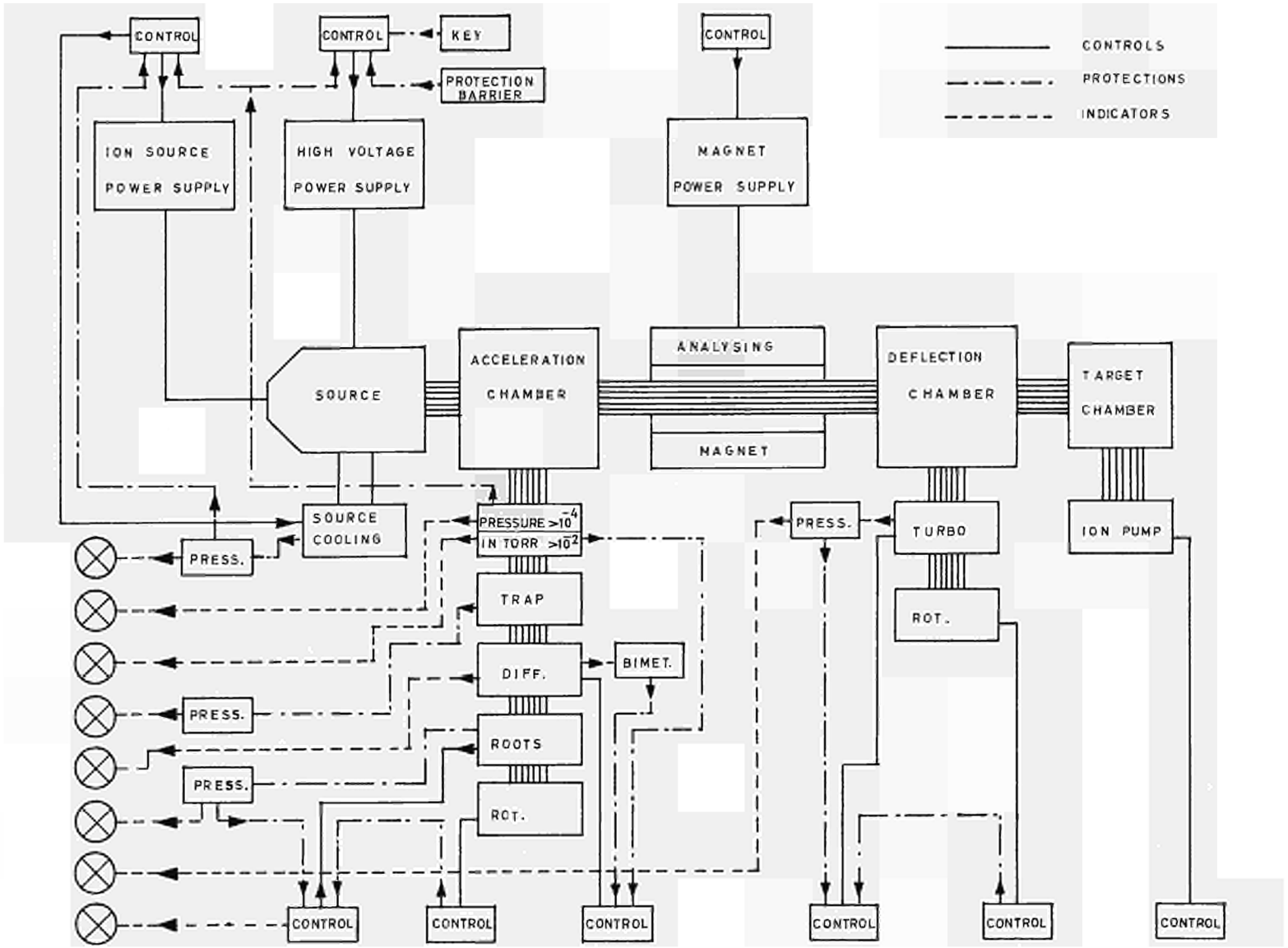

Fig 10.3 LOGIC OF THE MAIN PROTECTION CIRCUITS . SIMPLIFIED BLOCK DIAGRAM

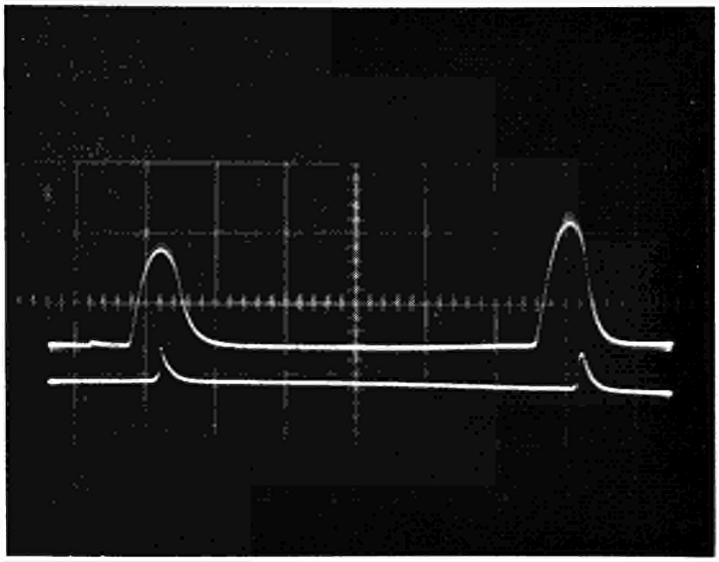

Fig. 10.4 Ion beam as displayed by the X-Y scanner.
The peaks in the lower part are due to the markers

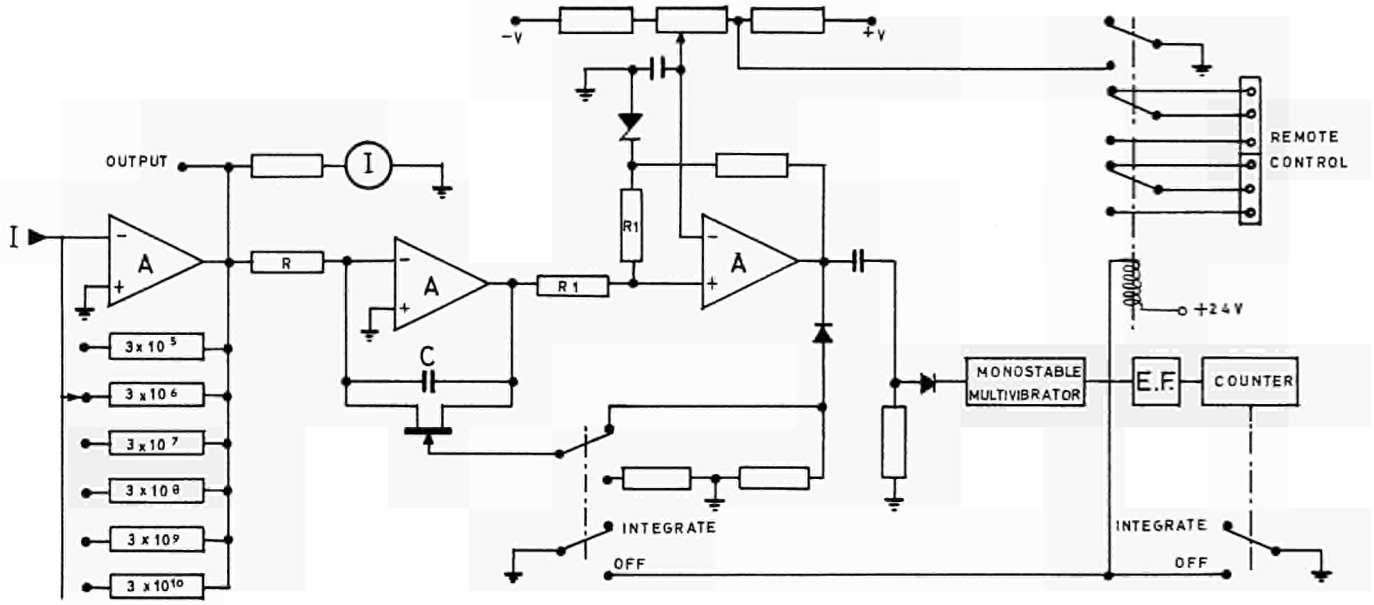

Fig. 10.5 CURRENT METER AND INTEGRATOR-SIMPLIFIED DIAGRAM

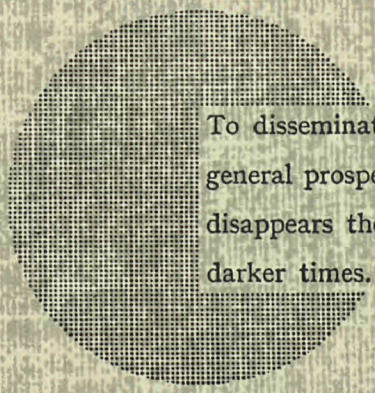

To disseminate knowledge is to disseminate prosperity — I mean general prosperity and not individual riches — and with prosperity disappears the greater part of the evil which is our heritage from darker times.

Alfred Nobel

SALES OFFICES

All reports published by the Commission of the European Communities are on sale at the offices listed below, at the prices given on the back of the front cover. When ordering, specify clearly the EUR number and the title of the report which are shown on the front cover.

OFFICE FOR OFFICIAL PUBLICATIONS OF THE EUROPEAN COMMUNITIES
P.O. Box 1003 - Luxembourg 1
(Compte chèque postal Nº 191-90)

BELGIQUE — BELGIË
MONITEUR BELGE
Rue de Louvain, 40-42 - B-1000 Bruxelles
BELGISCH STAATSBLAD
Leuvenseweg 40-42 - B-1000 Brussel

DEUTSCHLAND
VERLAG BUNDESANZEIGER
Postfach 108 006 - D-5 Köln 1

FRANCE
SERVICE DE VENTE EN FRANCE
DES PUBLICATIONS DES
COMMUNAUTÉS EUROPÉENNES
rue Desaix, 26 - F-75 Paris 15e

ITALIA
LIBRERIA DELLO STATO
Piazza G. Verdi, 10 - I-00198 Roma

LUXEMBOURG
OFFICE DES
PUBLICATIONS OFFICIELLES DES
COMMUNAUTÉS EUROPÉENNES
Case Postale 1003 - Luxembourg 1

NEDERLAND
STAATSDRUKKERIJ
en UITGEVERIJBEDRIJF
Christoffel Plantijnstraat - Den Haag

UNITED KINGDOM
H. M. STATIONERY OFFICE
P.O. Box 569 - London S.E.1

Commission of the
European Communities
D.G. XIII - C.I.D.
29, rue Aldringen
L u x e m b o u r g